COMMERCIAL DEMONSTRATION OF THE NOXSO SO_2/NO_x REMOVAL FLUE GAS CLEANUP SYSTEM

Contract No. DE-FC22-91PC90549

Quarterly Technical Progress Report No. 11

Submitted to

U.S. Department of Energy
Pittsburgh Energy Technology Center

September 1 through November 30, 1993

Project Definition Phase

U.S. DOE Patent Clearance Is Not Required Prior to the Publication of this Document

DISCLAIMER

Prepared by

Morrison Knudsen Corporation
Ferguson Division
1500 West 3rd Street
Cleveland, Ohio 44113-1406

Table of Contents

List of Figures

Figure **Page**

List of Tables

EXECUTIVE SUMMARY

The NOXSO process is a dry, post-combustion flue gas treatment technology which uses a regenerable sorbent to simultaneously adsorb sulfur dioxide (SO_2) and nitrogen oxides (NO_x) from the flue gas of a coal-fired utility boiler. In the process, the SO_2 is reduced to sulfur by-product (elemental sulfur, sulfuric acid, or liquid SO_2) and the NO_x is reduced to nitrogen and oxygen. It is predicted that the process can economically remove 90% of the acid rain precursor gases from the flue gas stream in a retrofit or new facility.

The objective of the NOXSO Demonstration Project is to design, construct, and operate a flue gas treatment system utilizing the NOXSO process. The effectiveness of the process will be demonstrated by achieving significant reductions in emissions of sulfur and nitrogen oxides. In addition, sufficient operating data will be obtained to confirm the process economics and provide a basis to guarantee performance on a commercial scale.

The project is presently in the project definition and preliminary design phase. Data obtained during pilot plant testing which was completed on July 30, 1993 is being incorporated in the design of the commercial size plant. A suitable host site to demonstrate the NOXSO process on a commercial scale is presently being sought.

Preliminary engineering studies provided information to decide on the basic plant arrangement. A scaled up POC design was selected as the general arrangement of choice based on a cost versus technical risk assessment. The other alternative being considered was a low profile design incorporating shop fabricated vessels and high temperature dense phase transport systems. It was concluded that the high temperature dense phase transport systems posed an unacceptable technical risk for a moderate overall cost savings. Subsequent efforts focused on reducing the height and cost of the scaled up POC design.

The first step in developing an adsorber computer simulation was completed. This included developing a numerical simulation procedure to solve the conservation and rate equations for diffusion and chemical reactions within the sorbent particle and conservation equations through the fixed bed. The reaction mechanisms were proposed and the appropriate rate constants and sorbent capacities calculated by matching experimental laboratory data.

Several processes for producing liquid SO_2 from the regenerator offgas were developed and evaluated. It was concluded that the Claus and burn process which involves making elemental sulfur as an intermediate product was the best choice.

The NOXSO process computer simulation was updated to include semi-plug solids flow through the fluidized beds of the sorbent heater and cooler. Heat loss calculations were also added.

Analysis of energy balances for the sorbent heater and cooler at the POC indicate a consistent lack of closure. It has been concluded that desorption of water in the sorbent heater and adsorption of water in the cooler is the most probable reason for this lack of closure.

1.0 INTRODUCTION

The NOXSO process is a dry, post-combustion flue gas treatment technology which uses a regenerable sorbent to simultaneously adsorb sulfur dioxide (SO_2) and nitrogen oxides (NO_x) from the flue gas of a coal-fired utility boiler. In the process, the SO_2 is converted to a sulfur by-product (elemental sulfur, sulfuric acid, or liquid SO_2) and the NO_x is reduced to nitrogen and oxygen. It is predicted that the process can economically remove 90% of the acid rain precursor gases from the flue gas stream in a retrofit or new facility.

Details of the NOXSO process are described with the aid of **Figure 1-1**. Flue gas from the power plant is drawn through a flue gas booster fan which forces the air through a two-stage fluid bed adsorber and centrifugal separator before passing to the power plant stack. Water is sprayed directly into one or both of the fluid beds as required to lower the temperature to 250-275°F by evaporative cooling. The fluid bed adsorber contains active NOXSO sorbent. The NOXSO sorbent is a 1.6 mm diameter γ-alumina bead impregnated with 5.2 weight % sodium. The centrifugal separator separates sorbent which may be entrained in the flue gas and returns it to the inlet of the dense phase transport system.

Spent sorbent from the adsorber flows into a dense-phase conveying system which lifts the sorbent to the top bed of the sorbent heater vessel. The sorbent flows through the multi-stage fluidized bed sorbent heater counter to the heating gas which heats the sorbent to the regeneration temperature of approximately 1150°F.

In the process of heating the sorbent, the NO_x is driven from the sorbent and carried to the power plant boiler in the NO_x recycle stream. The NO_x recycle stream is cooled from approximately 500°F to 150°F in the feedwater heater. This heater heats a slip stream of the power plants feedwater, thereby reducing the amount of extraction steam taken from the low pressure turbine, enabling the generation of additional electricity. The cooled NO_x recycle stream replaces a portion of the combustion air. The presence of NO_x in the combustion air suppresses the formation of NO_x in the boiler resulting in a net destruction of NO_x.

The heated sorbent enters the regenerator where it is contacted with natural gas. Through a series of chemical reactions, the sulfur on the sorbent combines with the methane and forms SO_2 and H_2S. Additional regeneration occurs in the steam treater section of the regenerator when the sorbent is contacted with steam converting the remaining sulfur on the sorbent to H_2S.

The regenerator offgas stream is directed to a sulfur recovery plant where the H_2S and SO_2 are converted to a sulfur by-product. Elemental sulfur, sulfuric acid, and liquid SO_2 are all potential end products from the regenerator offgas stream. Tail gas from the sulfur recovery plant will be incinerated and recycled back through the adsorbers to remove any sulfur compounds.

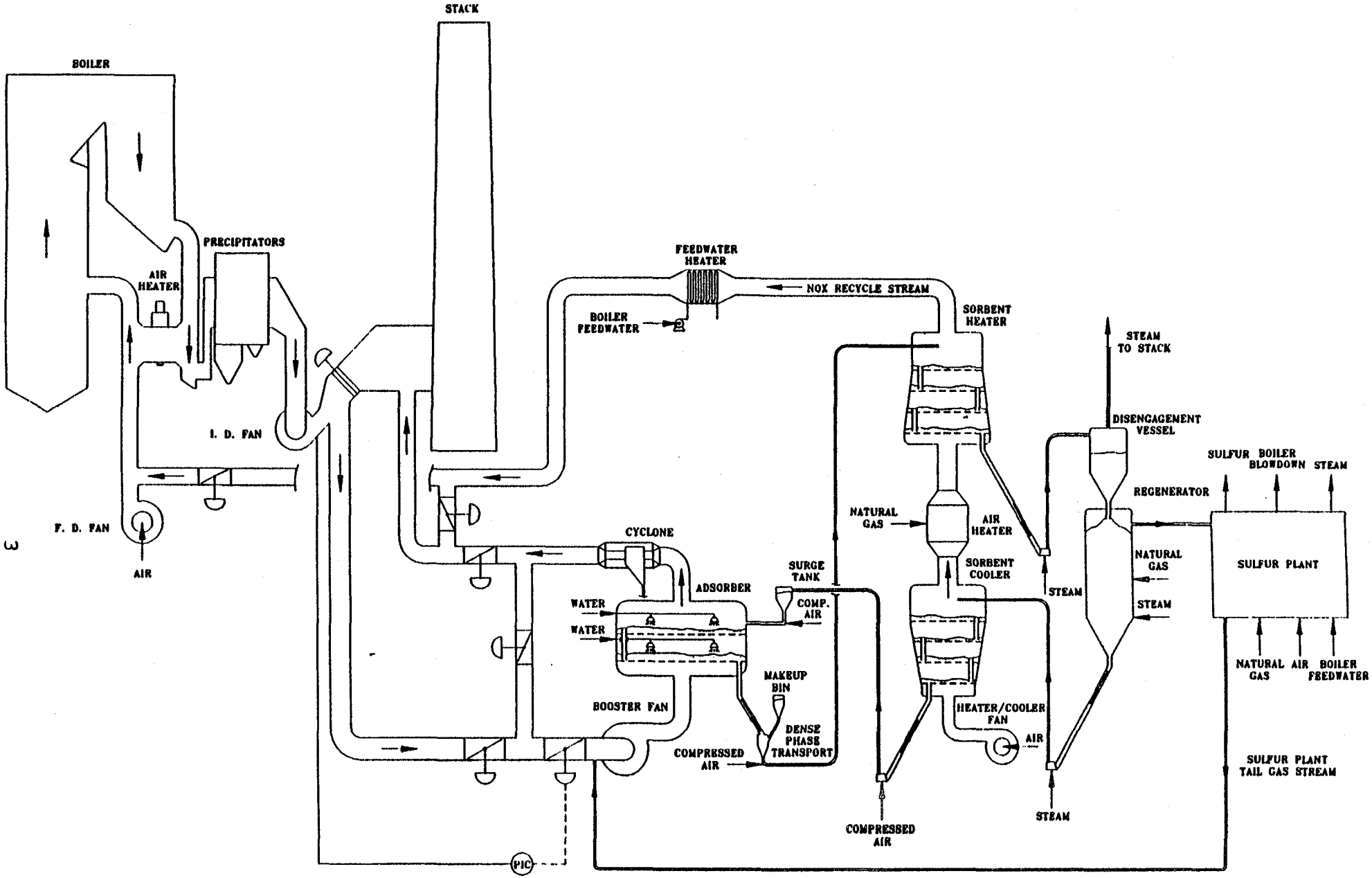

Figure 1-1. NOXSO Process Diagram

High temperature sorbent exiting the regenerator passes to the multi-stage fluidized bed sorbent cooler. The sorbent flows counter to the ambient air which cools the sorbent. Regenerated sorbent exits the cooler at 300°F. It is directed to the adsorber completing the sorbent cycle.

Ambient air which is forced through the sorbent cooler by the heater-cooler fan exits the sorbent cooler at approximately 900°F. This preheated air then enters the air heater where it is heated to approximately 1350°F so it is capable of heating the sorbent exiting the sorbent heater to 1150°F.

2.0 PROJECT DESCRIPTION

The objective of the NOXSO Demonstration Project is to design, construct, and operate a commercial scale flue gas treatment system utilizing the NOXSO process. The effectiveness of the process will be demonstrated by achieving significant reductions in emissions of sulfur and nitrogen oxides. In addition, sufficient operating data will be obtained to confirm the process economics and provide a basis to guarantee performance on a commercial scale.

3.0 PROJECT STATUS

The project is presently in the project definition and preliminary design phase. This phase was included in the project to allow completion of studies and preliminary activities which could be conducted in parallel with NOXSO's pilot plant project being conducted at Ohio Edison's Toronto Power Plant.

Testing at the pilot plant was completed on July 30, 1993. Performance at the pilot plant exceeded the design expectations for pollutant removal efficiency, sorbent attrition, and electrical power and natural gas consumption. The data continues to be evaluated and reduced to design equations which are used in the design of the commercial plant.

The search for a new host site continues. Two electric power generating facilities have submitted letters of intent expressing their interest to be the host site for the NOXSO process demonstration. Technical and financial issues regarding the execution of the project are being evaluated.

3.1 Project Management

Project management activities included the routine efforts of task assignments and information transfer within the project team comprised of personnel from NOXSO, MK-Ferguson, and W.R. Grace. Additionally, all DOE reports were submitted in accordance with the reporting requirements of the cooperative agreement. Significant effort was expended negotiating agreements necessary for the novation of the cooperative agreement from MK-Ferguson to NOXSO.

3.2 NEPA Compliance

No activities to satisfy the NEPA requirements were conducted this quarter. As soon as a new host site is identified, the EIV draft which was prepared for the host site at Ohio Edison's Niles Power Plant will be updated.

3.3 Preliminary Engineering

During this quarter, a decision to use the scaled up POC design was made. Although this plant is slightly more expensive than the low profile design, it poses less technical risk. Subsequent efforts focused on design alternatives to reduce the height and cost of the scaled up POC design.

3.3.1 Comparison of Scaled Up POC and Low Profile Design

Two different demonstration plant designs have been developed with cost estimates. The first design was a scaled up version of the POC plant. Vessel arrangement and sorbent transport was similar to the pilot plant. The cost estimate for this design was specific to Ohio Edison's Niles plant. The second design employed a low profile concept. All the vessels were located as close to the ground as possible, minimizing foundations and supporting structure while requiring the use of dense phase transport of sorbent between all vessels. The cost estimate for this plant was not site specific but was a generic battery limits estimate that did not include connections to the power plant.

The objective of the low profile design was to obtain a lower capital cost. To determine if the low profile design was less than the first design and to determine if the savings justified the risk of high temperature dense phase transport of sorbent, the two designs had to be compared on an equal basis. To accomplish this, costs required to build the low profile plant at Niles were added to the estimate for that design. The design effort put into the second design resulted in savings that could be applied to both plants. These savings included such things as reduced duct support foundations, lowering the duct work, a lower sulfur plant bid and less sulfur plant foundation, etc. These savings were deducted from the scaled up POC design. After several iterations, NOXSO and MK-Ferguson agreed on the cost estimate numbers. The result was that the low profile design saved between 2 and 3 million dollars. This savings was in the reduction of foundations and supporting structure and indirect costs as a result of a reduction in construction duration.

The low profile design requires the use of unproven high temperature dense phase transport in two places. If these high temperature dense phase transports do not operate properly and reliably, the demonstration project would be unsuccessful. NOXSO's conclusion is that the savings do not justify the risk.

The majority of savings attributable to the low profile design was in the area of foundations and structure. By modifying the scaled up POC design, similar savings can be realized. This can be accomplished by lowering the process tower as much as possible and making use of self supporting vessels. These design modifications are currently under investigation.

3.3.2 Steam Treater/Regenerator/Disengaging Vessel Sizing and Arrangement

The overall tower height in the original scaled-up NOXSO POC design was set by the dimensions of the vessels in the regeneration train (sorbent heater, sorbent cooler, regenerator, and steam treater) as well as the constraint that the sorbent discharge point from the sorbent heater be at the same elevation as the inlet to the regenerator and the discharge point from the steam treater be at the same elevation as the inlet to the sorbent cooler. Since the first scaled-up POC design was completed, several new developments have occurred. First, a disengaging vessel was added prior to the regenerator to separate the L-valve transport steam from the sorbent. This was done primarily to decrease the cost of the sulfur plant, but also serves the purpose of dampening flow fluctuations which should improve sulfur plant operability. Second, the possibility has been raised that the steam treater can either be eliminated completely from the design or combined with the regenerator into a single vessel. In the second case, no separate gas disengaging space would be provided for the steam treater portion of the regenerator. A third development was the possibility of getting a substantial lift out of the steam treater to sorbent cooler L-valve (hence forward the middle L-valve). The ability to achieve a substantial lift (where lift is defined as the difference between riser outlet and downcomer inlet elevations) makes possible new design schemes that will reduce the overall tower height. Coupled with options of eliminating the steam treater or combining the steam treater with the regenerator, height reductions of up to 40 feet may be achieved over the original scaled-up POC design. Design considerations and details of this new design are presented below.

Middle L-Valve Lift

The ability to reduce tower height is predicated on the assumption that a substantial lift can be achieved with the middle L-valve. Tests performed at the POC show that this is possible. When the dense phase lift at the POC was replaced by an L-valve, a lift of nearly 70 feet was achieved with a pressure differential of 11" H_2O between the downcomer inlet and the riser discharge points.

The pressure differential across the middle L-valve for the demonstration plant design is about 38" H_2O. The required lift is only about 25 feet. Therefore, the L-valve lift is certainly feasible. Required downcomer and riser dimensions as well as estimated gas flow rates for the middle L-valve will be the subject of a future study. For the purpose of this evaluation, it is sufficient to know that the middle L-vale lift is achievable.

Disengaging Vessel

The disengaging vessel was added to the NOXSO process to separate the top L-valve steam (sorbent heater to regenerator) from the regenerator offgas. The benefits of doing this include a less expensive sulfur plant because of the reduced volume of gas to be treated and higher conversions to elemental sulfur because of the lower water concentrations. In addition, the disengaging vessel will dampen flow fluctuations caused by the slugging nature of the L-valves.

Sizing the disengaging vessel is a tradeoff between two factors. On the one hand, it is desirable to minimize the sorbent residence time in the disengaging vessel so that temperature losses are kept to a minimum. On the other hand, because the standpipe between the disengaging vessel and regenerator provides a necessary gas seal, it is desirable to have a larger residence time allowing more flexibility in responding to upset conditions. In the current design, a vessel residence time of 20 minutes was used. During normal operations the vessel will operate at a level one half of full representing a 10 minute residence time.

The vessel volume is calculated based on a sorbent circulation rate of 330,820 lbs/h and the formula

$$V = m\,\tau/\rho$$

where
- m = sorbent circulation rate, lbs/h
- τ = sorbent residence time, h
- ρ = sorbent density, lbs/ft^3

There are an infinite number of combinations of vessel heights and diameters that will give the required volume. A few of these combinations are summarized in Table 3-1 with three different cone angles shown. The cylinder height and cone height do not sum to the total height because of the way cone height is defined. This is illustrated in **Figure 3-1**. The cone height is defined as L1. The vessel height, however, is measured from where the cone intersects the exit pipe. Therefore, for purposes of calculating the vessel height, the cone height is actually L1-L2.

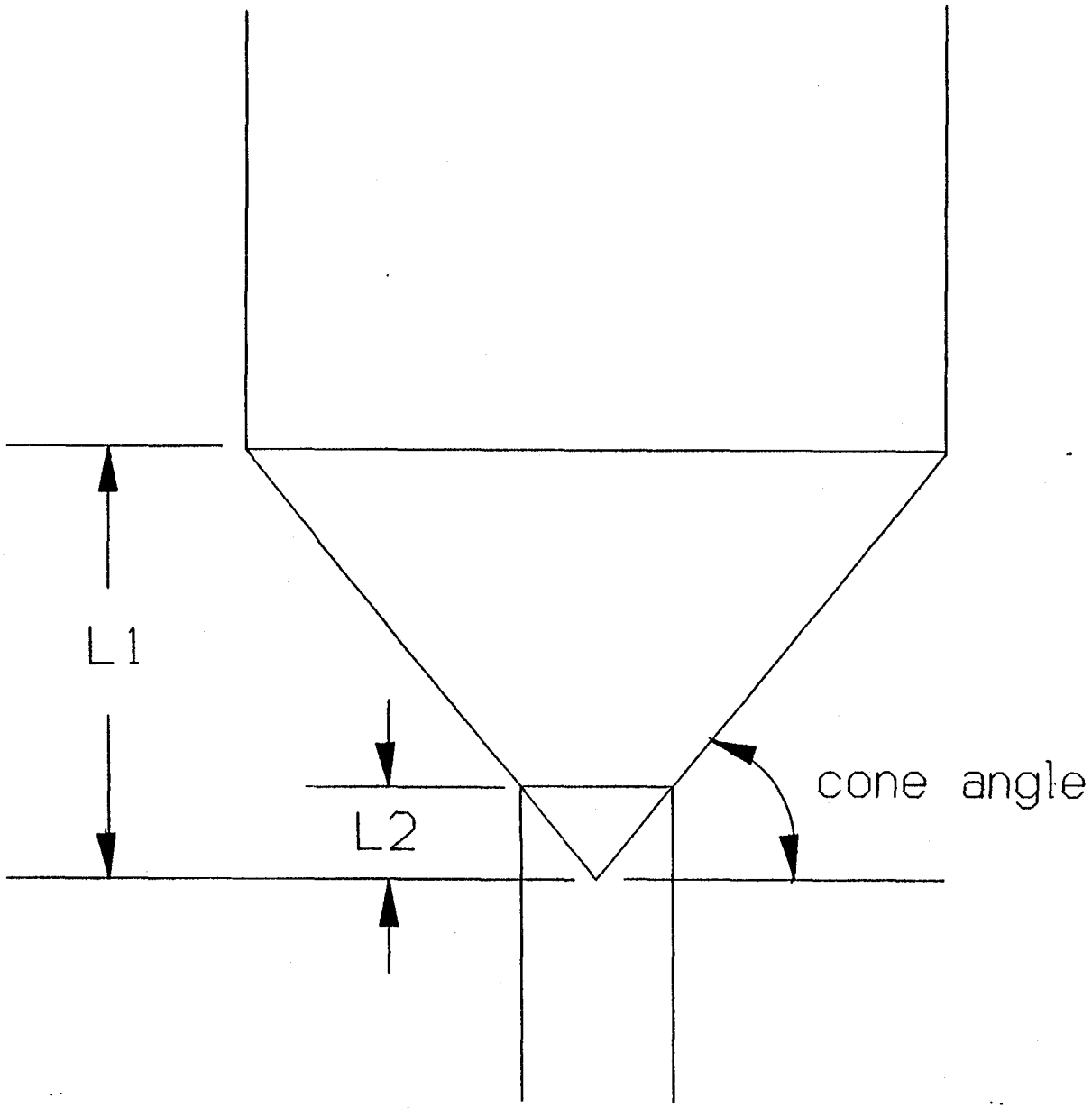

Figure 3-1. Differences in Cone Height and Vessel Height

Table 3-1. Disengaging Vessel Height and Diameter Combinations				
Cone Angle	**Inside Diameter (ft)**	**Cylinder Height (ft)**	**Cone Height (ft)**	**Total Height (ft)**
70°	14	14.1	19.2	30.6
	15	11.0	20.6	28.9
	18	4.15	24.7	26.1
60°	14	16.4	12.1	26.8
	15	13.5	13.0	24.8
	18	7.2	15.6	21.1
50°	14	17.7	8.3	24.9
	15	14.9	8.9	22.6
	18	8.8	10.7	18.3
	20	6.05	11.9	16.8
	22	3.9	13.1	15.8
	24	2.2	14.3	15.3
	26	0.75	15.5	15.1
	27.25	0	16.2	15.0

From Table 3-1 it can be seen that for a fixed diameter, the shallower the cone angle, the shorter the overall vessel height. Since there is no chemistry occurring in the disengaging vessel, the solids flow pattern is not critical. Therefore, the shallower angle of 50° was chosen. The vessel height also decreases as vessel diameter increases to the limit where the entire vessel is a cone. Above about 20 feet in diameter the height savings are minimal. Less than 2 feet reduction in height is realized for more than a 7 foot increase in diameter. The inside diameter chosen for this analysis was 18 feet.

Additional height must be added to the cylindrical portion of the vessel to account for lost volume due to the sorbents angle of repose as illustrated in **Figure 3-2**. An additional 1.75 feet was added to the vessel straight side to maintain a 20 minute residence time when the vessel is full. This assumes two sorbent inlet lines to the disengaging vessel and each discharging to half the distance to the center line.

A 36 inch diameter standpipe will be used to transfer sorbent from the disengaging vessel to the regenerator. The pressure differential across the standpipe will be used to control gas

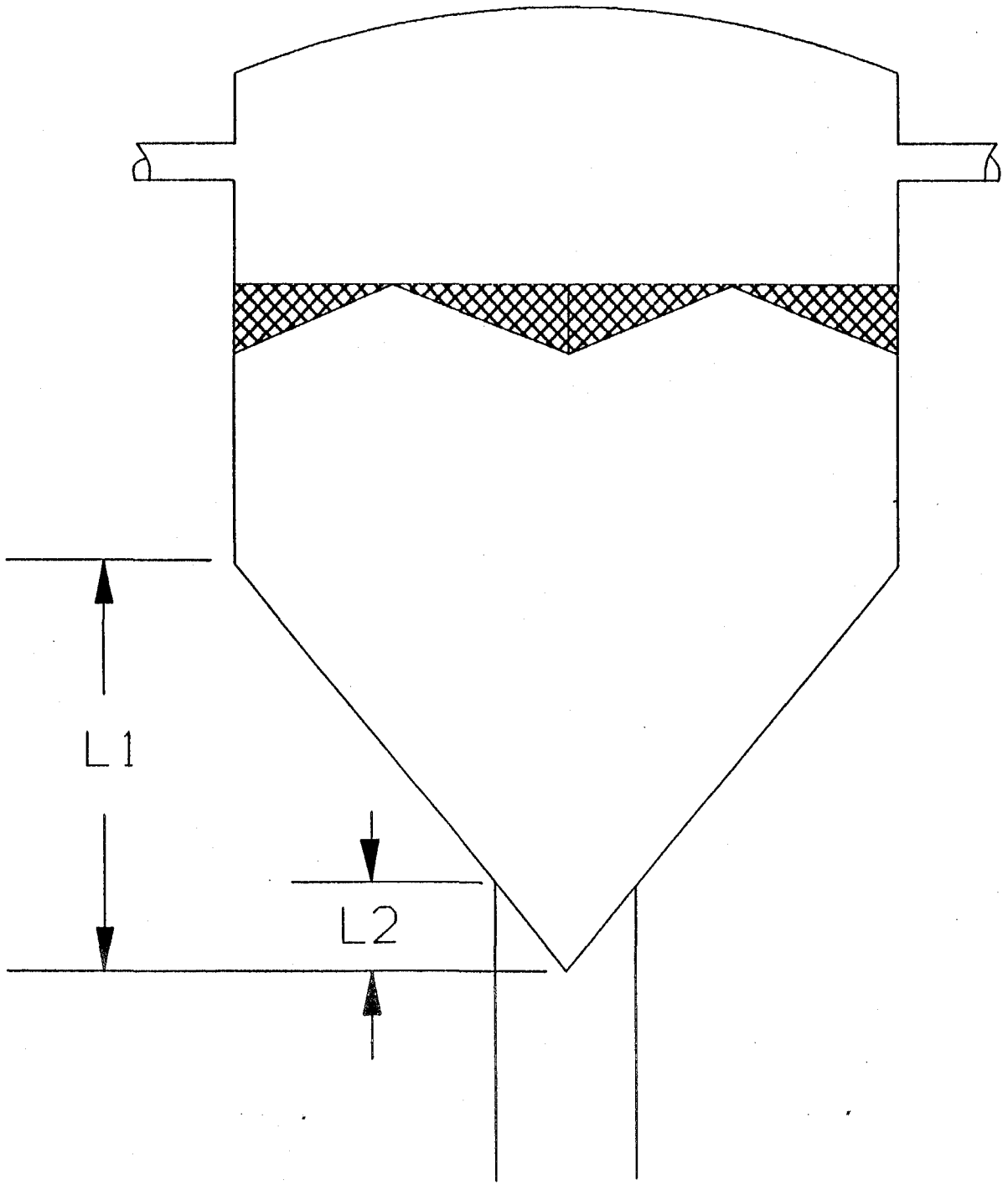

Figure 3-2. Lost Volume Due to Angle of Repose

transfer between vessels. During normal operation, the disengaging vessel will be controlled at a pressure 1-2" H_2O greater than the regenerator by using back pressure control on the steam vent line. This insures that a small amount of steam will purge downwards through the standpipe and prevent regenerator offgases from entering the disengaging vessel.

Regenerator

The regenerator vessel is used to contact sorbent with natural gas in a counter-current moving bed. The solids flow pattern in the regenerator is important so that a uniform solids residence time is maintained. This is done by using a steeper cone angle (60°) than was used in the disengaging vessel. The regenerator was sized to achieve a 50 minute residence time at the base case sorbent flow rate of 330,820 lbs/h. A residence time of nearly 46 minutes is achievable at a circulation rate 10% above the base case value. Table 3-2 shows combinations of vessel heights and diameters required to obtain the necessary sorbent volume. Seventy-five percent of the cone volume was considered to be active in process chemistry when determining volume requirements.

The sorbent L/D ratio is important in determining how well the gas will distribute in the moving bed. However, this ratio is much more critical in small diameter vessels. With the large vessel diameters used at the demonstration plant, and using concentric sparger rings to distribute the gas, smaller L/D ratios should work quite well.

A vessel inside diameter of 22 feet was chosen for this analysis. This gives a vessel height of about 42 feet after correcting the volume to account for the sorbents angle of repose. Also, it was assumed that the standpipe from the disengaging vessel to the regenerator will have a diameter of 36 inches and will be 5 feet long.

Table 3-2. Regenerator Vessel Height and Diameter Combinations

Cone angle	Inside Diameter (ft)	Cylinder Height (ft)	Cone Height (ft)	Total Height (ft)
60°	16	35.7	13.9	47.8
	18	27.1	15.6	41.0
	20	20.7	17.3	36.3
	22	15.95	19.1	33.3
	24	12.2	20.8	31.3

Steam Treater

For the case where a separate steam treater is used, a second 5 foot long standpipe will connect the regenerator to the steam treater. The steam treater vessel is used to contact the

sorbent with steam in a counter-current moving bed. Since the steam treatment step is not as critical as the methane treatment, a cone angle of 50° was once again used. Also, it was assumed that 80% of the cone volume is active in process chemistry. The steam treater was sized for a 15 minute residence time at a sorbent flow rate of 330, 820 lbs/h. Table 3-3 shows combinations of vessel heights and diameters required to accommodate the specified sorbent volume. Selecting an 18 foot diameter vessel and correcting the volume for the sorbents angle of repose and accounting for the 5 foot long standpipe, the steam treater vessel will be just over 25 feet high.

Table 3-3. Steam Treater Vessel Height and Diameter Combinations

Cone Angle	Inside Diameter (ft)	Cylinder Height (ft)	Cone Height (ft)	Total Height (ft)
50°	14	13.1	8.3	20.3
	16	9.2	9.5	17.5
	18	6.4	10.7	15.9
	20	4.35	11.9	15.1

Potential Height Reductions

Assuming that the sorbent heater, air heater, and sorbent cooler will remain in a stacked configuration, the maximum potential height reduction is determined by how much these vessels can be compressed. In the current scaled-up POC design, there is 74 feet between the top of the sorbent cooler and the bottom of the sorbent heater. Assuming that 10 feet of ductwork is required above the sorbent cooler to accommodate the air bypass line, an additional 10 feet is required between the air heater and sorbent heater, and that the air heater occupies 14 feet between the vessels then 40 feet can be removed from between the sorbent heater and sorbent cooler. Currently, the bottom of the duct leading to the sorbent cooler is 11 feet above ground level. Assuming this duct could be moved to grade, an additional 10 feet can be removed from the sorbent heater/sorbent cooler train. Therefore, the maximum possible reduction in tower height is 50 feet.

Case 1

The first case examined assumes that all three vessels (disengaging, regenerator, and steam treater) are required. **Figure 3-3** is a sketch of the proposed configuration. If the base of the middle L-valve is located at ground level, the sorbent inlet to the disengaging vessel would be about 113½ feet above grade. This sets the elevation of the sorbent heater sorbent outlet. By lowering the sorbent heater to this new elevation, 30 of the possible 40 feet could be removed from between the sorbent heater and sorbent cooler. The new elevations are indicated on the NOXSO process tower drawing of the full height plant shown in **Figure 3-4**.

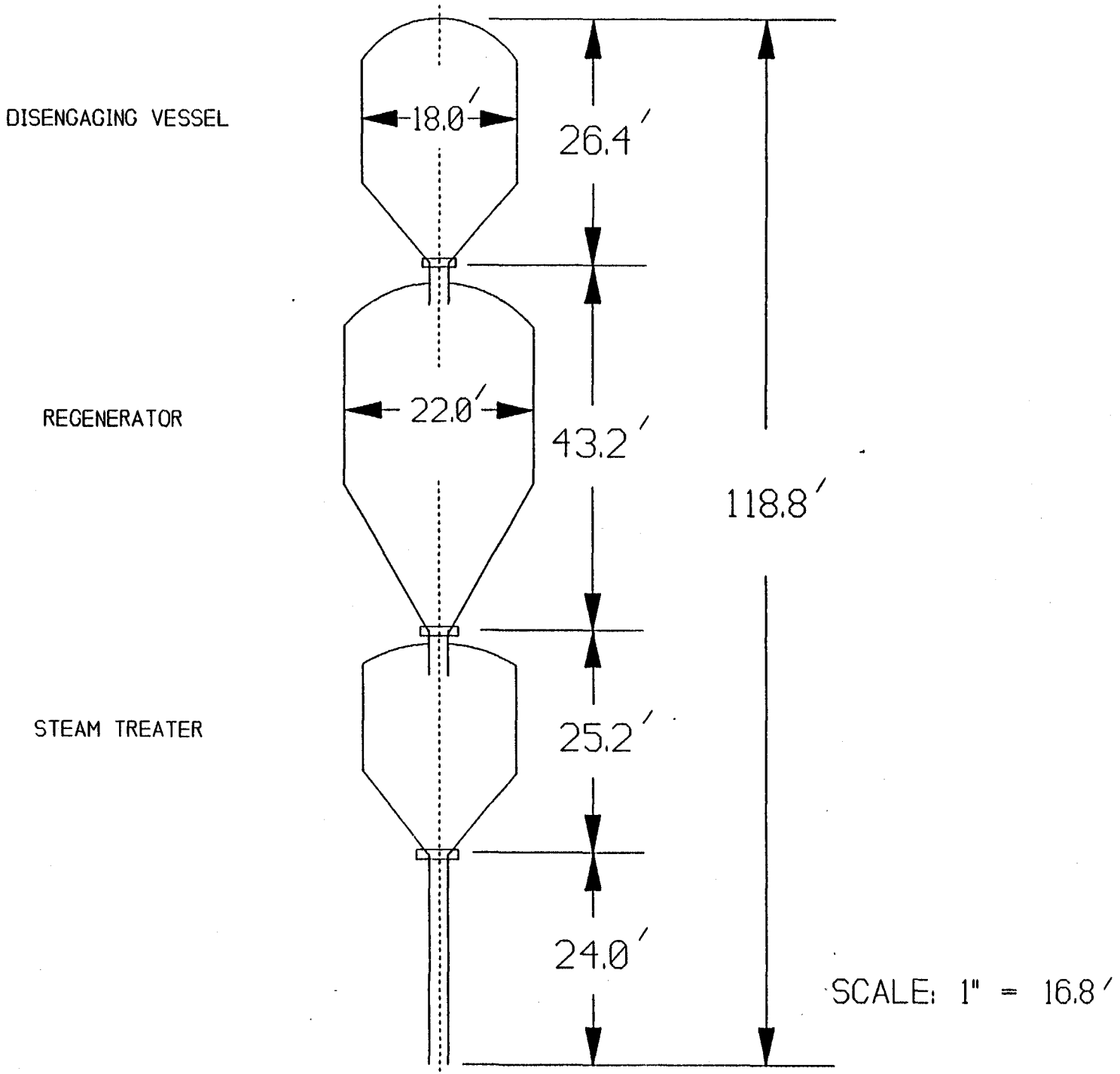

Figure 3-3. Scale Drawing of Regeneration Train

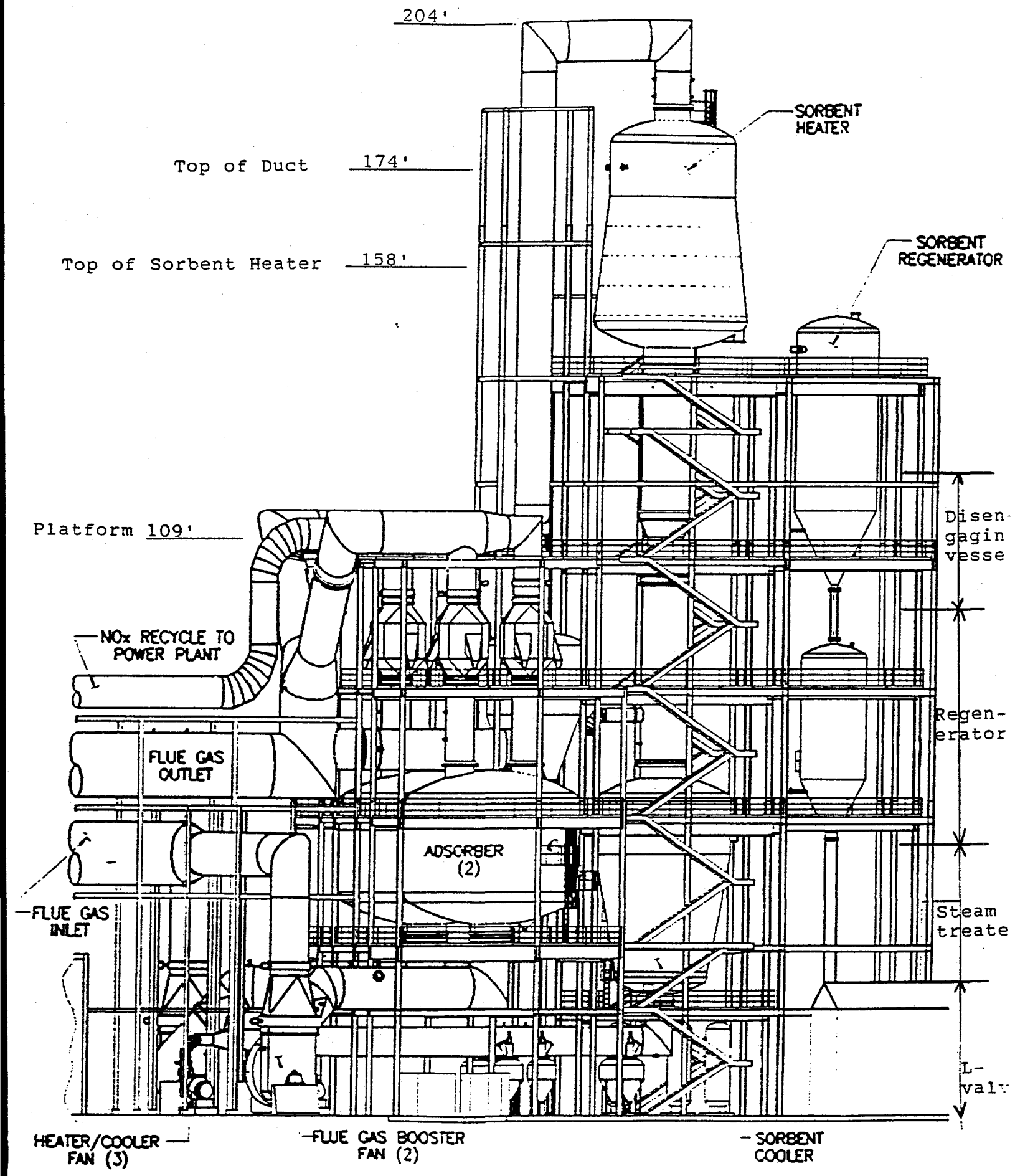

Figure 3-4. NOXSO Process Tower

To further decrease the tower height, a portion of the middle L-valve could be located below grade. Assuming the bottom 10 feet is underground, the new elevations for the top of the sorbent heater offgas duct, the top of the sorbent heater and the top platform would be 164 feet, 148 feet, and 99 feet respectively.

Case 2

The second case examined assumes that the steam treater can be combined with the regenerator in a single vessel with no separate gas disengaging space for the steam treater. The elevations for this arrangement are shown in **Figure 3-5**. In this case, the bottom of the middle L-valve is at grade, and the maximum 50 feet is removed from the sorbent heater/sorbent cooler train. The top of the sorbent heater would be 138 feet above grade and the top platform would be 89 feet above grade. The middle L-valve would be required to give a 20 foot lift.

Case 3

The third case examined assumes that the steam treater can be eliminated completely without adding extra volume to the regenerator. However, this case only reduces the disengaging vessel/regenerator height by 5 feet over the combined regenerator/steam treater case (case 2). Since the maximum height reduction of 50 feet was already achieved in case 2, there is not significant incentive to eliminate the steam treater entirely.

Summary

The design considerations used to size the disengaging vessel, regenerator, and steam treater are summarized in Table 3-4. The sorbent circulation rate was assumed to be 330,820 lbs/h which leads to a 1.2 wt% sulfur gain in the adsorber.

Table 3-4. Vessel Design Considerations

	Disengaging Vessel	Regenerator	Steam Treater
Maximum residence time (min)*	20	50	15
Cone angle	50	60	50
Sorbent volume (ft^3)	3150	7880	2360
Inside Diameter (ft)	18	22	18

*Based on the base case sorbent flow rate.

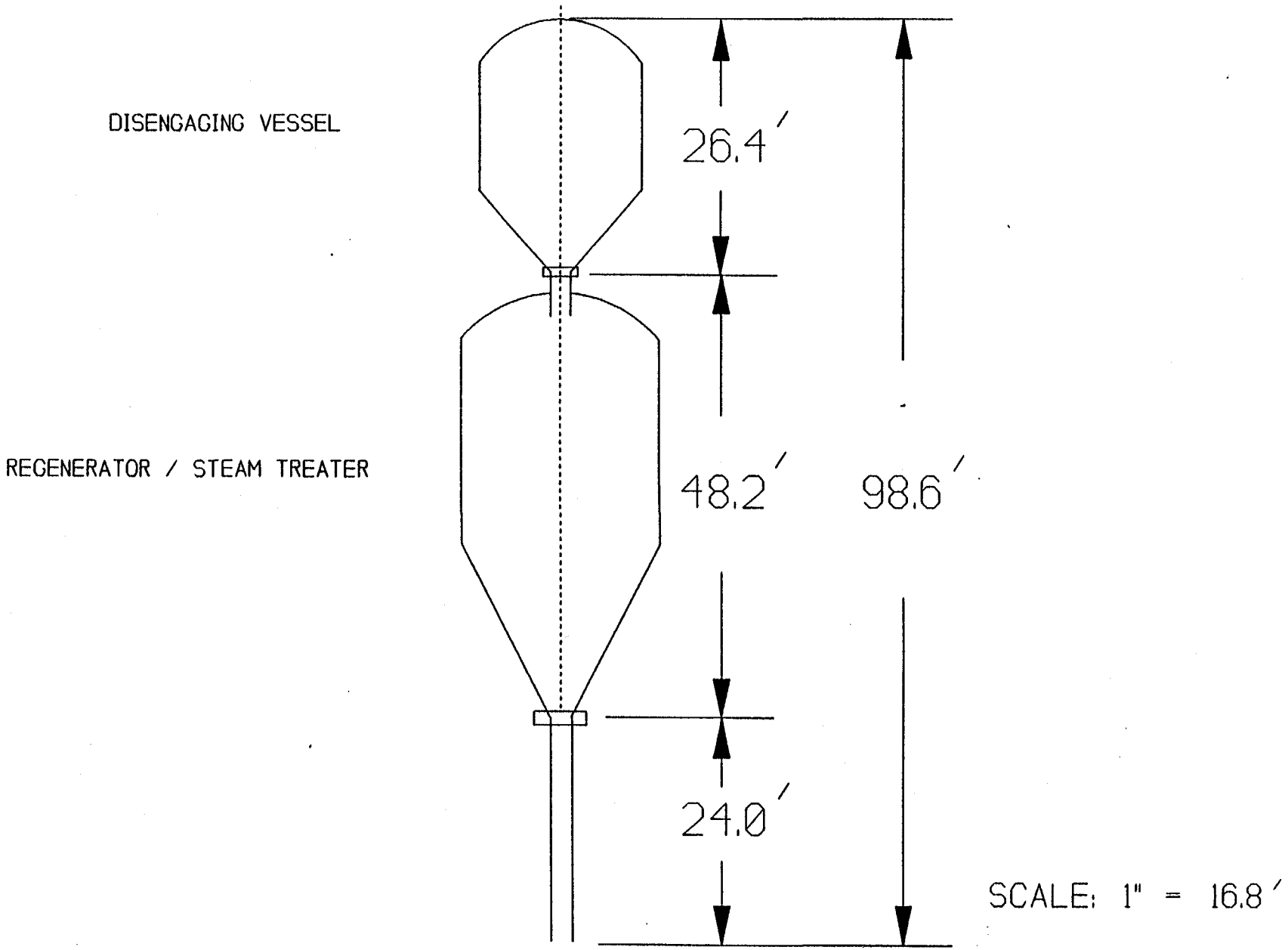

Figure 3-5. Sketch of Regenerator/Steam Treater System

The potential tower height reductions are summarized in Table 3-5.

Table 3-5. Potential Height Reductions of Scaled-up POC Design

	Disengaging Vessel	Regenerator	Steam Treater	L-Valve	Height Reduction
Case 1	Yes	Yes	Yes	At grade	30 ft
Case 1a	Yes	Yes	Yes	10 ft below grade	40 ft
Case 2	Yes	Yes	combined w/ regenerator	at grade	50 ft
Case 3	Yes	Yes	No	at grade	50 ft

The current demonstration plant design is based on Case 2. POC testing indicated that steam treatment of the sorbent may not be required at all. However, since only a small increase in vessel size is required to provide space for steam treatment, and because no additional height advantages are gained by eliminating steam treatment entirely, Case 2 is the best configuration for the regenerator.

3.4 Nitrogen Oxide Studies

No nitrogen oxide studies were conducted during this reporting period.

3.5 Process Studies

Process study activities focused on aspects of the NOXSO process which can reduce the operating cost, increase the pollutant removal efficiency, or reduce the technical risk of the demonstration project. These studies are conducted using a combination of theoretical analysis, analysis of pilot plant data, and laboratory experiments.

3.5.1 Adsorber Model

Fixed-Bed Computer Simulation Program

Coupling the governing equations of the fixed-bed reactor (presented in Quarterly Technical Report No. 10) with appropriate reaction rate equations forms the basis for the computer simulation. A collocation method was used to solve the diffusion-reaction equations for the solid phase. A Runge-kutta method was used to solve the continuity and energy equations for the gas phase. To verify the computer program, an analytic solution of the first order gas and zero-th order solid reaction (M. Ishida and C.Y. Wen, "Comparison of Kinetic and

Diffusional Models for Solid-Gas Reactions", AIChE Journal, vol.14, No. 2, p.311, 1968) was compared with the computer results. **Figure 3-6** shows the comparison, which is perfect. The Thiele module shown on the Figure is equal to R $(K/D_e)^{1/2}$, in which R = particle radius, K = reaction rate constant, and D_e = effective gas diffusity. As the reaction proceeds, the outer-layer of solid reactant eventually exhausts. This phenomena transforms the solid phase from a single diffusion-reaction layer to one ash and one diffusion-reaction layer. Only diffusion occurs in the ash layer. If the initial solid component is not uniformly distributed, say outer layer has a higher concentration than the center, the solid phase will become three layers: one ash layer in the outer, one ash layer in the center, and one diffusion-reaction layer in between. The boundaries of layers move as reactions proceed. To solve the solid phase rigorously, one has to deal with multiple moving boundaries. For single gas and single solid components, this type of problem was addressed by many researchers, but none for multi-components. Instead of chasing the mathematical elegance, we decided to approximate the multi-layer moving-boundary problem with the solution obtained from a single lay fixed-boundary problem. This decision is made from the practical point of view. The sorption reaction of NOXSO process is very complicated, involving the formation and destruction of many solid components. To track the moving boundary for each solid component requires a lot of computation time. Considering the accuracy of the experimental data, and the errors in estimating the transport properties, the return may be limited. The approximation is made by increasing the number of nodes for the collocation, and by forcing the negative solid concentration to be zero. A comparison between the analytic solution (Ishida and Wen, ibid) of one ash and one diffusion-reaction layers with the approximation result is shown in **Figure 3-7**. Both solid and gas concentration profiles show significant difference between the one lay and two layers approaches. But the computed solid conversion is very close, i.e. 0.992 versus 0.982 for the analytic and approximated solution, respectively. The small difference is caused by the following reasons: (1) the solid concentration of simulation is almost parallel to that of the analytic solution, and (2) the difference occurs mainly at the center of the solid, which has a smaller radius than the entire solid particle. **Figure 3-8** shows the result for approximating an unevenly distributed initial-solid concentration. Although the approximation result may not reflect the real situation, **Figure 3-8** shows the existence of two ash layers and one diffusion-reaction layer in between.

Because the diffusion-reaction problem is dependent upon the Thiele modulus, the error caused by the approximation would be different at various Thiele modulus. Table 3-1 of M.P. Dudukovic and H.S. Lamba's paper ("Solution of Moving Boundary Problems for Gas-Solid Noncatalytic Reactions by Orthogonal Collocation", Chemical Engineering Science, vol.33, p.303, 1978) contains the solid conversion data for different Thiele modulus. Since Dudukovic and Lamba also used the collocation method for their computer simulation program, their results gauge our approximation method. The comparison between the two-layer solutions and the one layer approximation is listed in Table 3-6. The results shown in **Figures 3-6** through **3-8** are for spherical particles, and those listed in Table 3-6 are for slabs. In both cases, our program used a Sherwood number = 10^6 to account for the gas-solid interface mass transfer. Table 3-6 shows that the approximation solution under-predicts the solid conversion, when the dimensionless time is greater than 1. Dimensionless time = 1 corresponds to the onset of the ash layer. Using more node points in the collocation gives a better simulation result, but the

Figure 3-6.

One diffusion-reaction layer

Thiele module = 5. at time= 1.

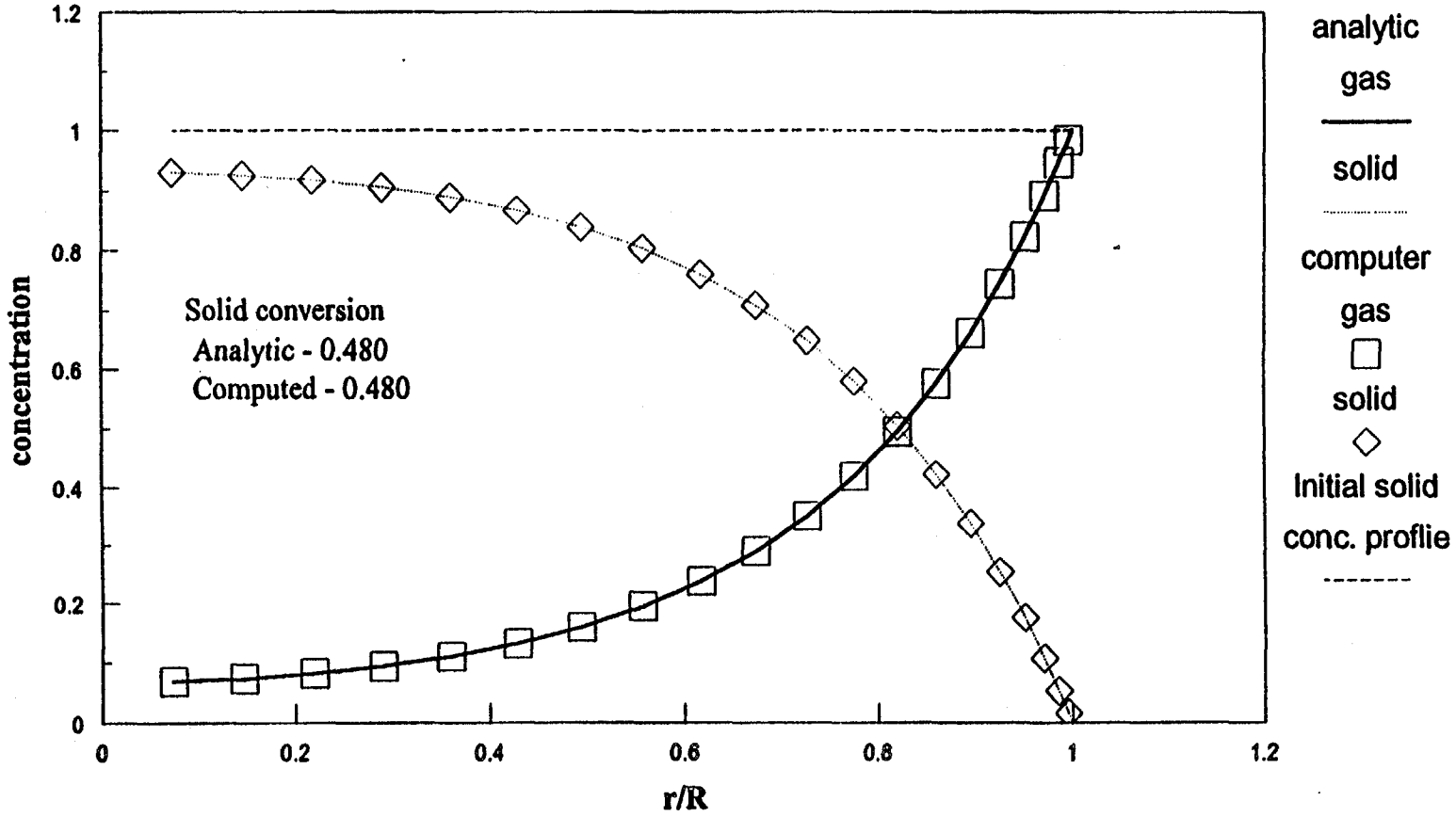

c:\may94\fixbed\gsrxn0.cht

Figure 3-7.

One ash and one diffusion-reaction layers

Thiele module = 5. at time= 4.5

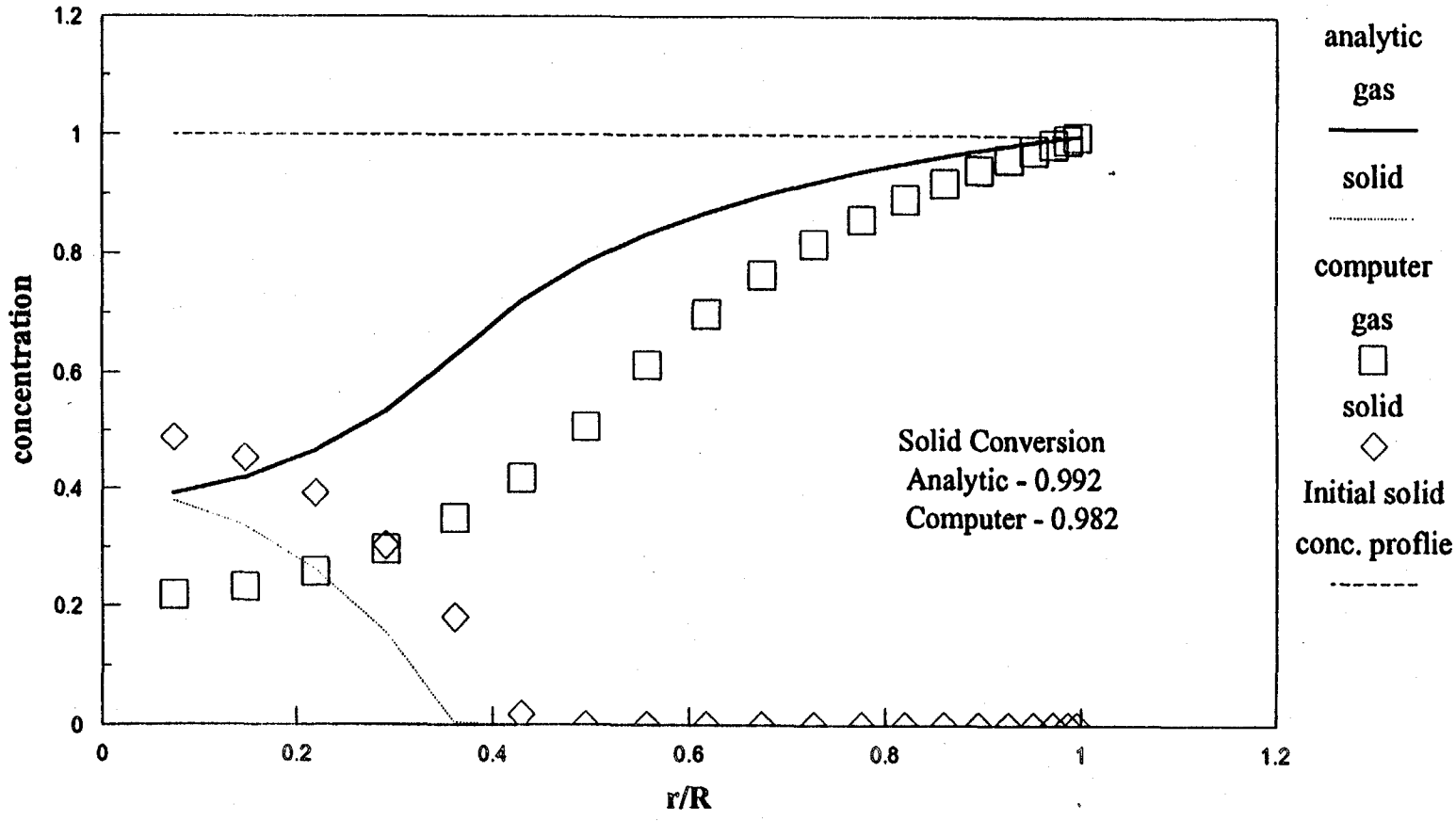

c:\may94\fixbed\gsrxn1.cht

Figure 3-8.

Two ash and one diffusion-reaction layers

Thiele module = 5. at time= 2.0

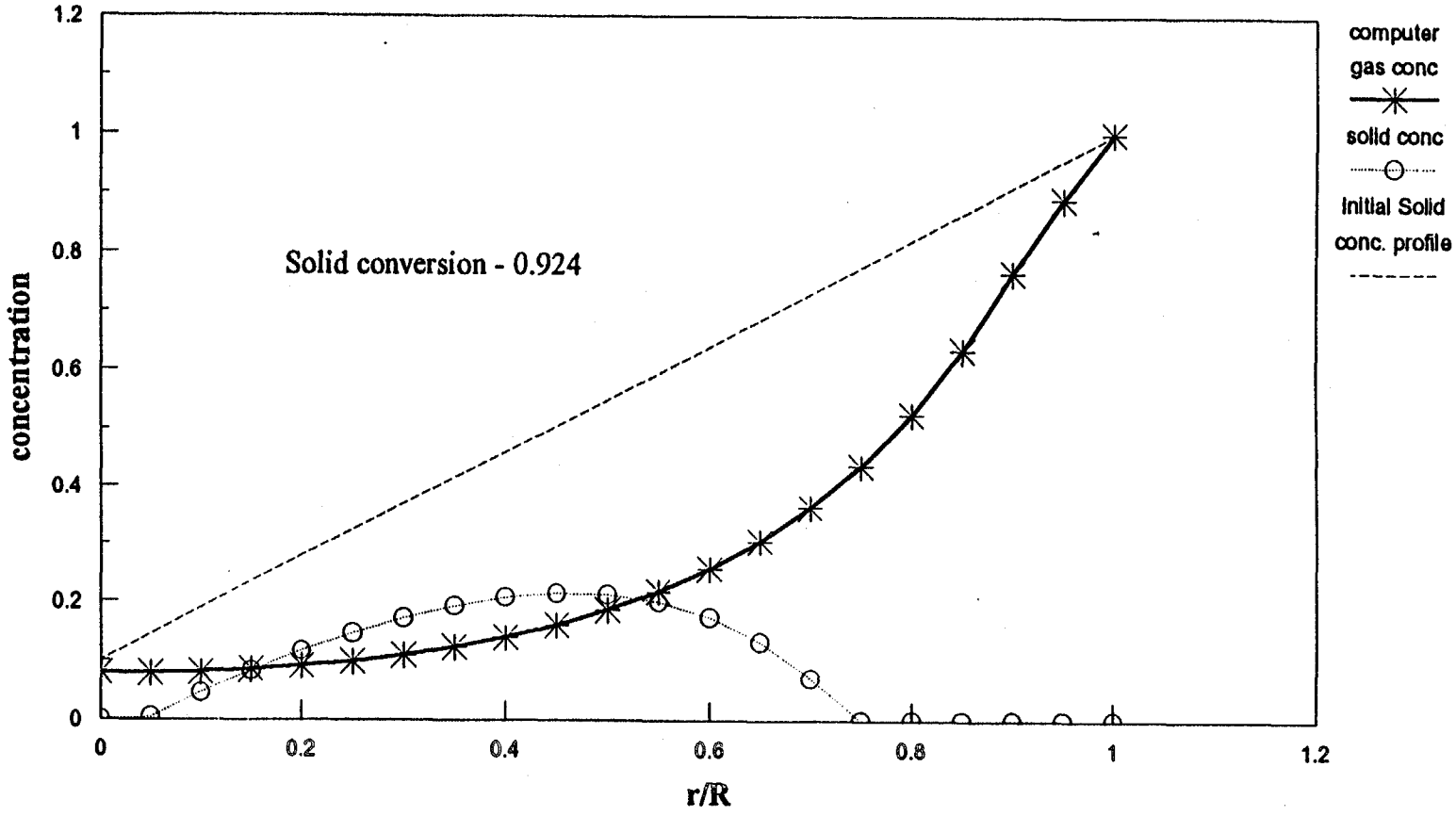

c:\may94\fixbed\gsrxn2.cht

return is diminished when the number of node points exceeds ten. In the worst case, the approximation introduces a less than 4% error, which is acceptable as compared to the error associated with experiments and the estimation of transport coefficients. Similar to the Dudukovic and Lamba's results, our approximation solutions require more node points to closely simulate high Thiele-modulus cases. The appropriate node number for simulating the NOXSO sorption was determined by comparing the sum of error square obtained from the simulation and observation data. The sum of error square decreased when the node number was increased from three to five. But no significant improvement was found with ten nodes. After judging the diminished return between the accuracy and computer time, five nodes were used in the later computation.

Table 3-6. Comparison of Two-layer Model Results with One-layer Approximation Solution for a Slab.

Thiele Modulus	Dimension-less Time	Analytical Solution	Dudukovic and Lamba's Two-layer Model		One-layer approximation			
			3-nodes	8-nodes	3-nodes	8-nodes	10-nodes	20-nodes
1	0.2	0.152319	0.152318	0.152320	0.152319	0.152319	0.152319	0.152319
1	0.7	0.533116	0.533113	0.533120	0.533116	0.533116	0.533116	0.533116
1	1.1	0.831613	0.831612	0.831618	0.831402	0.831402	0.831402	0.831402
1	1.3	0.939326	0.939327	0.939330	0.938376	0.937477	0.937730	0.937915
1	1.4	0.977439	0.977441	0.977450	0.974435	0.974539	0.975749	0.975705
5	1.0	0.199982	0.196192	0.199982	0.200004	0.199986	0.199986	0.199986
5	3.0	0.447117	0.451096	0.447117	0.454458	0.427668	0.432057	0.429329
5	7.0	0.720180	0.726106	0.720179	0.710010	0.694982	0.687315	0.684730
5	10.0	0.868172	0.873393	0.868171	0.859126	0.838421	0.828384	0.827146
5	13.0	0.986027	0.989824	0.986025	0.920049	0.959376	0.939199	0.939963
10	1.0	0.100000	0.0857363	0.0999994	0.103699	0.100033	0.100033	0.100033
10	5.0	0.300000	0.326479	0.300002	0.319520	0.278868	0.289245	0.289409
10	15.0	0.538516	0.584218	0.531517	0.520541	0.417745	0.520548	0.524682
10	30.0	0.768080	0.810456	0.768081	0.849173	0.756112	0.740604	0.749944
10	47.0	0.962803	0.995466	0.962803	0.872133	0.948148	0.947490	0.942644
25	1.0	0.040000	--	0.0397580	0.073457	0.040549	0.040460	0.040455
25	30.0	0.307246	--	0.309014	0.761237	0.344798	0.325389	0.306538
25	60.0	0.436348	--	0.438026	0.856161	0.510642	0.458769	0.429877
25	100.	0.564269	--	0.565681	0.949187	0.700500	0.595316	0.559112

NOXSO Sorption Chemistry

The NOXSO sorbent is prepared by spraying Na_2CO_3 solution on the surface of δ-alumina spheres. Both sodium ion and alumina contribute to the NOXSO sorbent's capacity to adsorb SO_2 and NO_x from flue gas. The sorption reaction is very complicated. It involves many steps of surface reactions. Instead of searching for the controlling rate step, we use a molecular

reaction scheme to explain the offgas concentration profile observed in a fixed-bed adsorption test. The use of a molecular reaction scheme is well illustrated by G.F. Froment in his studies of thermal cracking for ethane, propane, butane, and their mixtures. (K.M. Sundaram and G.F. Froment, "Model of Thermal Cracking Kinetics-I, II", Chemical Engineering Science, vol.32, p.601, p.609, 1977).

The reaction of alumina is described as follows:

$$SO_2 + Al(1) \rightarrow Al.SO_2 \quad (1)$$
$$NO + Al(2) \rightarrow Al.NO \quad (2)$$
$$NO_2 + Al(3) \rightarrow Al.NO_2 \quad (3)$$
$$Al.NO + SO_2 + 0.5\ O_2 \rightarrow Al.SO_2 + NO_2 \quad (4)$$

Different reaction sites on the alumina, Al (1), Al (2), Al(3), were assigned to SO_2, NO, NO_2 respectively. The adequacy of these assignments later verified with the observed data. Using the different site approach leaves us more adjustable parameters to fit the data. Later discussion shows that reaction (3) is not necessary.

Similar to the reactions of alumina, we assume the reactions of sodium are as follows:

$$(5)\ SO_2 + Na_2O(1) + 0.5\ O_2 \rightarrow Na_2SO_4 \quad (5)$$
$$(6)\ SO_2 + NO + 1.5\ Na_2O(1) + 1.25\ O_2 \rightarrow Na_2SO_4 + NaNO_3 \quad (6)$$
$$(7)\ SO_2 + NO + Na_2O(1) + O_2 \rightarrow Na_2SO_4 + NO_2 \quad (7)$$
$$(8)\ 3NO_2 + Na_2O(2) \rightarrow 2NaNO_3 + NO \quad (8)$$
$$(9)\ 2NaNO_3 + SO_2 \rightarrow Na_2SO_4 + 2NO_2 \quad (9)$$

The reason why SO_2 and NO_2 react on different sodium sites $Na_2O(1)$ and $Na_2O(2)$ is not known, but the different site approach is needed to fit the experimental data. This will be discussed later. Basically, reactions (6) and (7) carry the same reactants. Reaction (6) implies that NO and SO_2 are competing for the same sodium sites, while the reaction (7) says sodium only reacts with SO_2 and converts NO to NO_2. There is no obvious way to prove which is the dominant reaction. To make the reaction scheme complete, we include both reactions. The comparison between the simulation and observation data will give us a clue to select the right one. Later discussions show that reaction (7) can be neglected.

NOXSO knew that oxygen and steam in the flue gas enhances the NO_x and SO_2 sorption on the sorbent. Since water is not included in the reactions, the Na_2O and Al shown in reactions (1) through (9) stand for the hydrolyzed sodium and alumina. This implication simplifies the reaction equations. The entire reaction scheme was proposed from our laboratory observations, which include,

1. The sorbent removes little NO when there is no SO_2 in the flue gas.
2. The adsorbed NO_x will desorb from the sorbent if more SO_2 is fed into the reactor. This phenomena was observed on the tests using either NOXSO sorbent or sorbent substrate only.

3. The desorbed NO_x is mainly NO_2
4. The spent sorbent, when heated to desorb all the NO_x but not treated with regenerants to remove sulfur, losses its NO_x removal ability.
5. The NO_x and SO_2 sorption reaction is NO_x sorption limited.

Reactions (5) and (6) indicate that sodium was consumed by SO_2 and NO. The NO sorption was caused by its reaction with SO_2 and Na_2O. Reactions (4), and (7) through (9) explain the formation and removal of NO_2 for sodium and alumina.

Reaction Rate Form

NOXSO studies show that the effects of water vapor and oxygen concentrations on sorption vanishes at high concentration. Water losses its effect when its concentration exceeds 3%. And the oxygen becomes fruitless when its concentration is greater than 1%. A typical PC-boiler flue gas contains 8% water and 4% oxygen. Since NOXSO process sprays water into the flue gas to lower its temperature, the water content in the flue gas will be higher than the regular flue gas. Also, air leaked through the air preheater increases the flue gas oxygen concentration. For example, the oxygen content of the POC plant's flue gas varied from 8 to 10% depending on the load. The water and oxygen concentrations are in excess, and do not effect the NO_x and SO_2 sorption rates. To simplify the simulation task, we assume all the reaction rates are first order with respect to each reactant component. The first-order assumption is selected for its simplicity.

(1) $-d[SO_2]/dt = k1[SO_2][Al(1)]$
(2) $-d[NO]/dt = k2[NO][Al(2)]$
(3) $-d[NO_2]/dt = k3[NO_2][Al(3)]$
(4) $-d[SO_2]/dt = k4[SO_2][Al.NO]$
(5) $-d[SO_2]/dt = k5[SO_2][Na_2O(1)]$
(6) $-d[SO_2]/dt = k6[SO_2][NO][Na_2O(1)]$
(7) $-d[NO]/dt = k7[SO_2][NO][Na_2O(1)]$
(8) $-d[NO_2]/dt = k8[NO_2][Na_2O(2)]$
(9) $-d[SO_2]/dt = k9[SO_2][NaNO_3]$

Transport Coefficients

All the transport coefficients were calculated according to chapter three of G.F. Froment and K.B. Bischoff's "Chemical Reactor Analysis and Design" (1st edition, 1979, John Wiley and Sons). A random pore model is chosen to describe the sorbent internal structure, which takes the macro and micro pore volume, and pore radius into account. The unknown gas properties were estimated according to R.C. Reid, J.M. Prausnitz, and T.K. Sherwood's "The Properties of Gases and Liquids" (3rd edition, 1977, McGRAW-HILL).

Simulation of the Fixed-bed Adsorption Test to Determine the Reaction Rate Constant

The purpose of developing the fixed-bed simulation program is to determine the global reaction rate constants to explain the observed offgas concentration profiles. The global rate constant is different from the local rate constant. The latter is determined by using a differential reactor, the former is obtained by an integral reactor. The differential reactor method is very popular for obtaining the rate constants for the catalytic reaction because of the constant nature of the catalyst. But for non-catalytic gas-solid reaction, both gas and solid components are changing. It is hard to represent the entire reaction history using local rate constant. The data obtained form the integral reactor becomes useful in determining the global rate constant. Based on this concept, a trial and error method was used to determine these rate constants. The computer gives a trial offgas concentration based on the known operating condition and the guessed rate constants. The trial profile was then compared with the observed profile and the difference was used to adjust the rate constants. A Marquest optimization routine was used to find the best rate constants.

Totally, there are 14 parameters, nine rate constants plus three alumina sites and two sodium sites. To ensure the quality of the fit, we sequentially determine the parameter values through a series of laboratory tests. All the tests were conducted at 120°C using aged POC-40 sorbent with 5 slpm gas flowrate.

The objective of the first sorption test was to obtain the information about the SO_2 sorption. Thirty gram of POC-40 sorbent was used to treat the flue gas containing 4300 ppm SO_2, 8% H_2O, 10% O_2 with balanced N_2 in an integral reactor. Since neither NO nor NO_2 exist, the fit between the observation and simulation will reveal the rate constants of the SO_2 reactions, i.e. k1, k5 and the SO_2 sorption sites, i.e. Al(1) and $Na_2O(1)$. The comparison between the simulation and the experimental data is shown in **Figure 3-9**. The fit is excellent. The importance of each parameter is evaluated by changing their values one at a time. We found that the fit is almost insensitive to the value of $Na_2O(1)$. Since the amount of sodium is a measurable quantity, the $Na_2O(1)$ becomes a known value. The value of $Na_2O(1)$ is set equal to the measured sodium content in the later simulation. According to the simulation results, the alumina sorption is much faster than sodium sorption. After 20 minutes, the alumina sites are completely exhausted. The best-fit parameter values are listed in Table 3-7.

The second sorption test was designed to obtain the information about the NO and NO_2 sorption. Fifty grams of POC-40 sorbent was used to treat the flue gas of 89.7 ppm NO, 791 ppm NO_2 with balanced N_2. Since no SO_2 participates in the test, the fit between the observation and simulation will give the rate constants of k2 and k8, and the NO and NO_2 sorption sites, Al(2), Al(3), and $Na_2O(2)$. The comparison between the simulation and the experimental data is shown in **Figure 3-10**. The fit is remarkable. Since the fit is insensitive to the presence of Al(3), we decided to drop the reaction (3) in the later simulation. The best fit results are also listed in Table 3-7. It should be pointed out that the fit is very sensitive to the $Na_2O(2)$ value. The best-fit value is 1.18 wt% as compared to the measured 5 wt% sodium. Due to the small $Na_2O(2)$ value we add the reverse of reaction (8) into our reaction scheme. Hopefully, the reversible reaction will increase the $Na_2O(2)$'s value. But adding the reverse reaction merely

Figure 3-9.

30g POC-40 sorbent @120C fixed-bed adsorption

test: 5 slpm (4300ppmSO2 + 8%H2O + 10%O2 + N2)

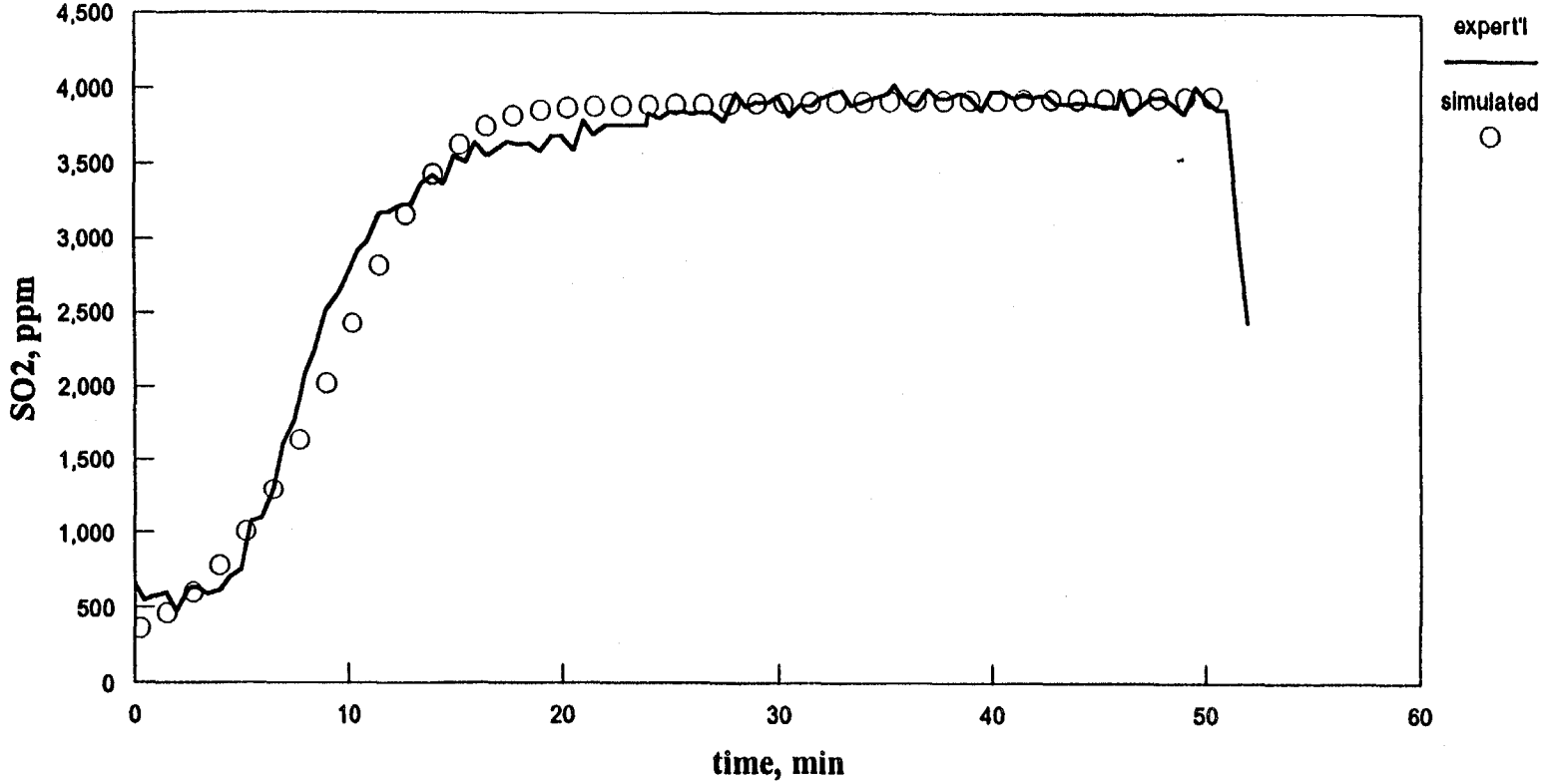

c:\may94\fixbed\ads\dos\nly120SO.cht

k1=5.46054, k6=674.3241, Na=2.69655, Al=0.76654

SS=0.35987, nl=41, tsec=15, nodes=5

Figure 3-10.

50g POC-40 sorbent @120C fixed-bed adsorption

test: 5 slpm (89.7ppm NO + 791ppm NO2 + N2)

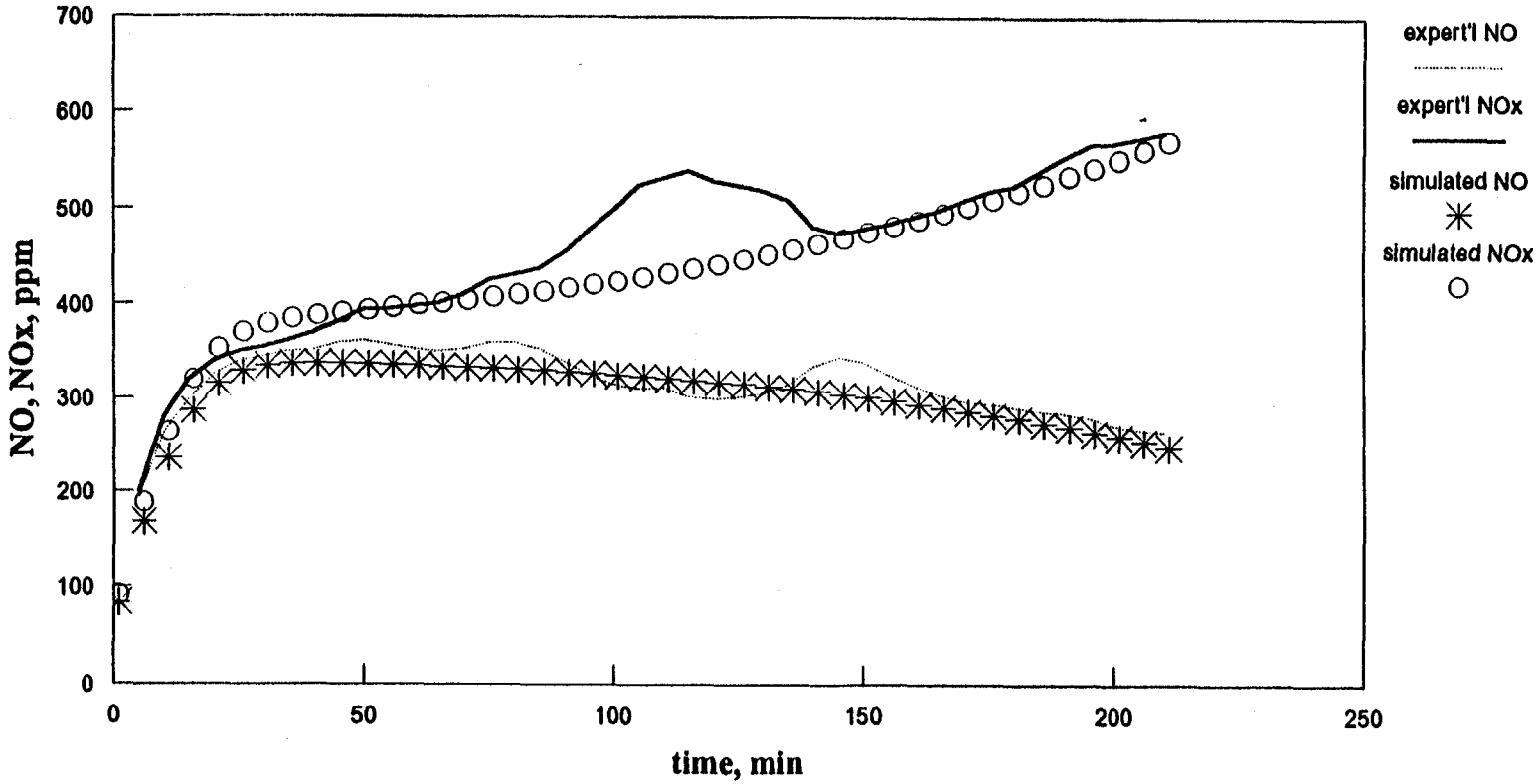

c:\may94\fixbed\ads\dos\nly120NO.cht

k4=317.26, k7=2210.85 Na=1.467 Al=0.028

k8=1.3576d4, Aln2=0.021776 (K8,Aln2 adjustable)

reduces the forward reaction rate. Since no better explanation is available, we assume the sodium has different sorption sites for NO_2 and SO_2. Similar to the SO_2 sorption, the simulation result indicates that the alumina sorption is much faster than sodium. After 20 minutes, the alumina sites are completely spent.

After these two tests are complete, only four unknowns remain, i.e. k4, k6, k7, and k9. A real flue gas test will enable us to determine these unknown rate constants. Therefore,the third test was conducted to simulate the real flue gas. Thirty grams of POC-40 sorbent was used to treat the flue gas containing 2400 ppm SO_2, 950 ppm NO_x, 2% O_2, 8% H_2O and balanced N_2. The inlet NO_2 to NO_x ratio of the inlet gas was assumed to be 5% because only the NO_x concentration was reported. The fit result for the NO and NO_x at the beginning of the test is horrible. The only way to fit the initial NO and NO_x curve is to increase the amount of Al(2). This adjustment is reasonable from the chemistry point of view. As mentioned before, water vapor and oxygen increase the sorbent reactivity. The Al(2) value was determined by the second test with no H_2O and O_2. Reactions (6) and (7) were used either together or separately in the simulation. From the fit result we found that including reaction (7) lowers the NO profile. Therefore reaction (7) was deleted from the scheme in the final simulation. The final fit is shown in **Figure 3-11**. The fit is satisfactory.

Table 3-7. Parameters for 120°C Adsorption Simulation

Parameters	SO_2 only test	NO and NO_2 only test	SO_2 and NO_x test
Al(1)	0.752		
Al(2)		0.028	0.55
Al(3)		not needed	
$Na_2O(1)$	5		
$Na_2O(2)$		1.18	
k1	681.2		
k2		2211	
k3		not needed	
k4			50
k5	2.646		
k6			$7X10^8$
k7			not needed
k8		317.3	
k9			104

Figure 3-11.

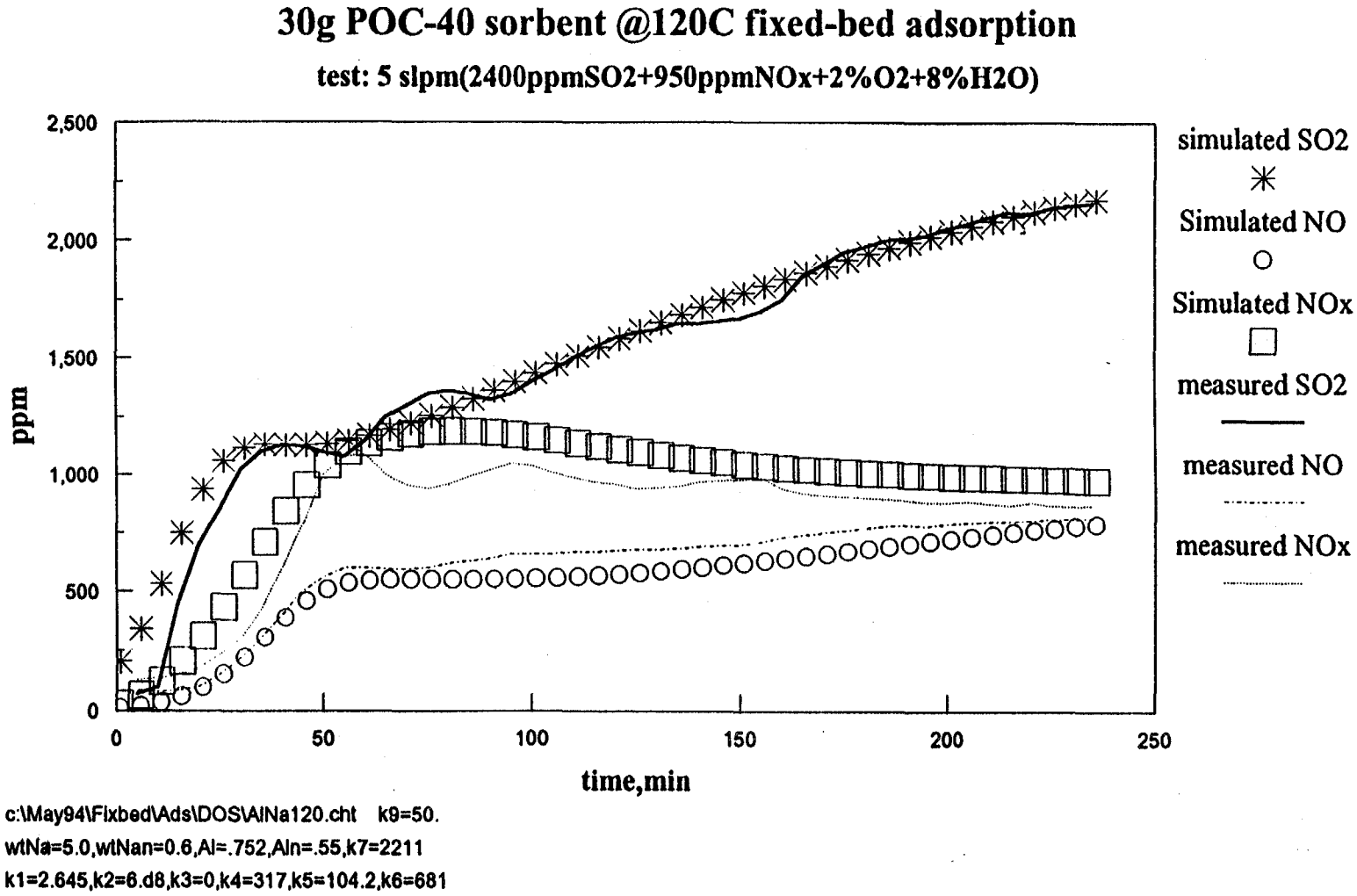
30g POC-40 sorbent @120C fixed-bed adsorption
test: 5 slpm(2400ppmSO2+950ppmNOx+2%O2+8%H2O)
2,500
2,000
1,500
1,000
500
0
ppm
0
50
100
150
200
250
time,min
simulated SO2
Simulated NO
Simulated NOx
measured SO2
measured NO
measured NOx
c:\May94\Fixbed\Ads\DOS\AlNa120.cht k9=50.
wtNa=5.0,wtNan=0.6,Al=.752,Aln=.55,k7=2211
k1=2.645,k2=6.d8,k3=0,k4=317,k5=104.2,k6=681

Gas and Solid Concentration Profiles Inside the Sorbent Pellet

One advantage of having a computer simulation program is to allow us to visualize the reaction situation inside the sorbent pellet without using any costly instruments. The gas and solid concentration profiles at different reaction times the reactor inlet are shown in **Figures 3-12** through **3-18**. These figures are based on the third test condition.

Figures 3-12 through **3-15** show the gas concentration profile across the pellet. The concentration at r/R=1.1 stand for the bulk gas concentration. After five minutes of sorption, NO and SO_2 show steep concentration profiles (**Figure 3-12**). And NO_2 has a flat profile. Similar profiles were observed after 15 minutes (**Figure 3-13**). However, the situation changes after 30 minutes (**Figure 3-14**). SO_2 still possesses a steep profile, but NO's becomes flat, and NO_2 builds up. The trend becomes clear after 45 minutes (**Figure 3-15**). The corresponding solid concentration profiles are shown in **Figures 3-16** through **3-18**. These plots show the build up and decline of Na_2SO_4 and $Na_2O(1)$ along the radius. The important message is about the formation and destruction of the $NaNO_3$ with time. At 15 minutes, (**Figure 3-16**), the $NaNO_3$ has an increasing concentration profile with the radius, but the profile reverses at 45 minutes (**Figure 3-18**). The reversed profile indicates the SO_2 has already driven NO_2 out of the $NaNO_3$. Therefore, a flat $NaNO_3$ profile corresponds to the maximum NO capacity before SO_2 attacks the $NaNO_3$ to form additional NO_2. **Figure 3-17** shows that the flat $NaNO_3$ profile occurs at about 30 minutes of sorption. At the same time, the eighth reaction (NO_2 removed by $Na_2O(2)$) just barely started.

Conclusion

NOXSO sorption reactions were selected by comparing the experimental data with computer simulation results. The reactions are listed in the following:

(1) $SO_2 + Al(1) \rightarrow Al.SO_2$
(2) $NO + Al(2) \rightarrow Al.NO$
(4) $Al.NO + SO_2 + 0.5\ O_2 \rightarrow Al.SO_2 + NO_2$
(5) $SO_2 + Na_2O(1) + 0.5\ O_2 \rightarrow Na_2SO_4$
(6) $SO_2 + NO + 1.5\ Na_2O(1) + 1.25\ O_2 \rightarrow Na_2SO_4 + NaNO_3$
(8) $3NO_2 + Na_2O(2) \rightarrow 2NaNO_3 + NO$
(9) $2NaNO_3 + SO_2 \rightarrow Na_2SO_4 + 2NO_2$

Based on the simulated adsorption results, we found that sorption on the alumina is much faster than on sodium. The SO_2 and NO_x breakthrough is due to exhausting alumina sorption sites. The gas concentration profile inside the sorbent indicates that the sorption is diffusion limited for the entire SO_2 sorption. But NO has a shifting control mechanism. Initially, NO sorption is diffusion limited and later becomes reaction limited.

Figure 3-12.

Gas concentration inside the sorbent

(after 5 min)

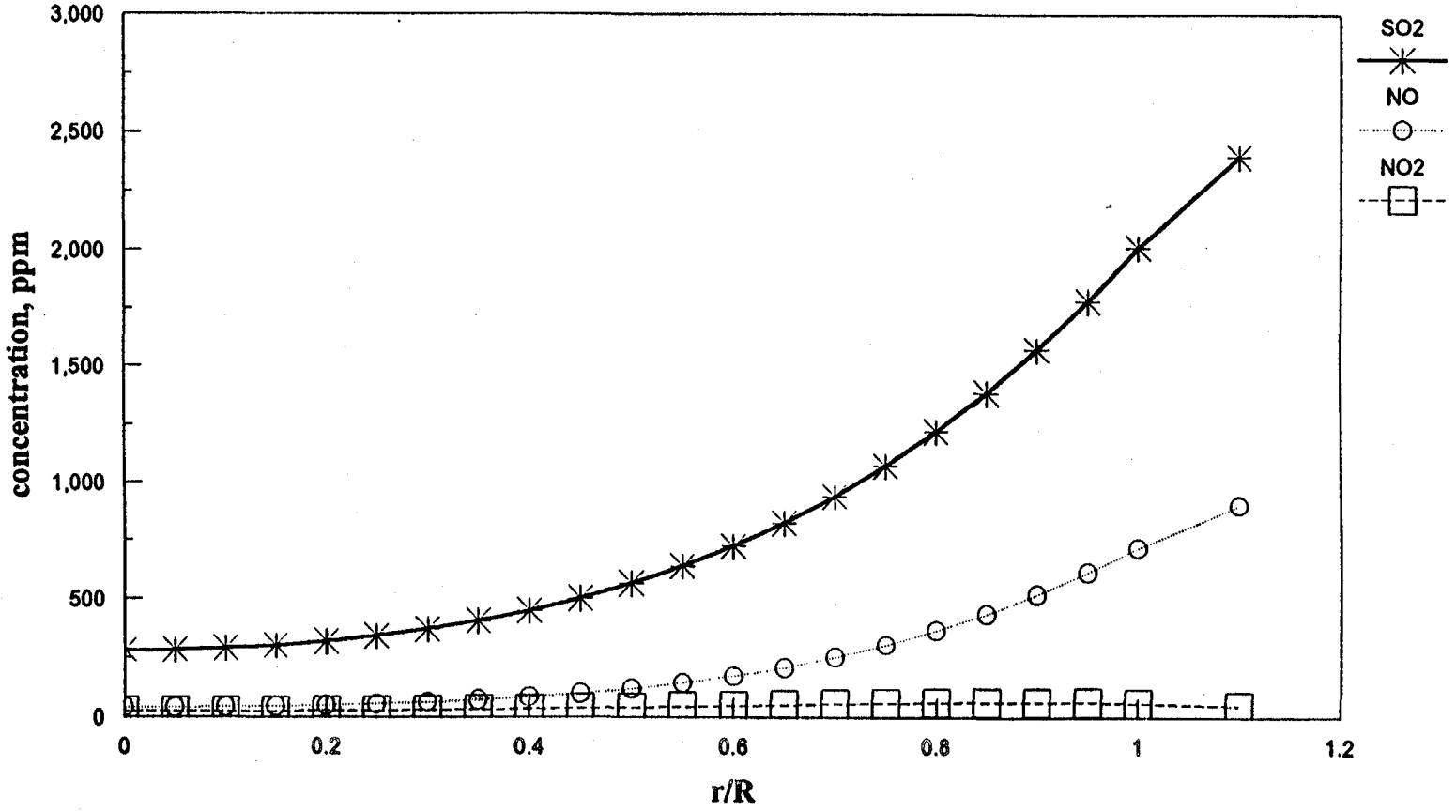

Figure 3-13

Gas concentration profile inside the sorbent

(after 15 min)

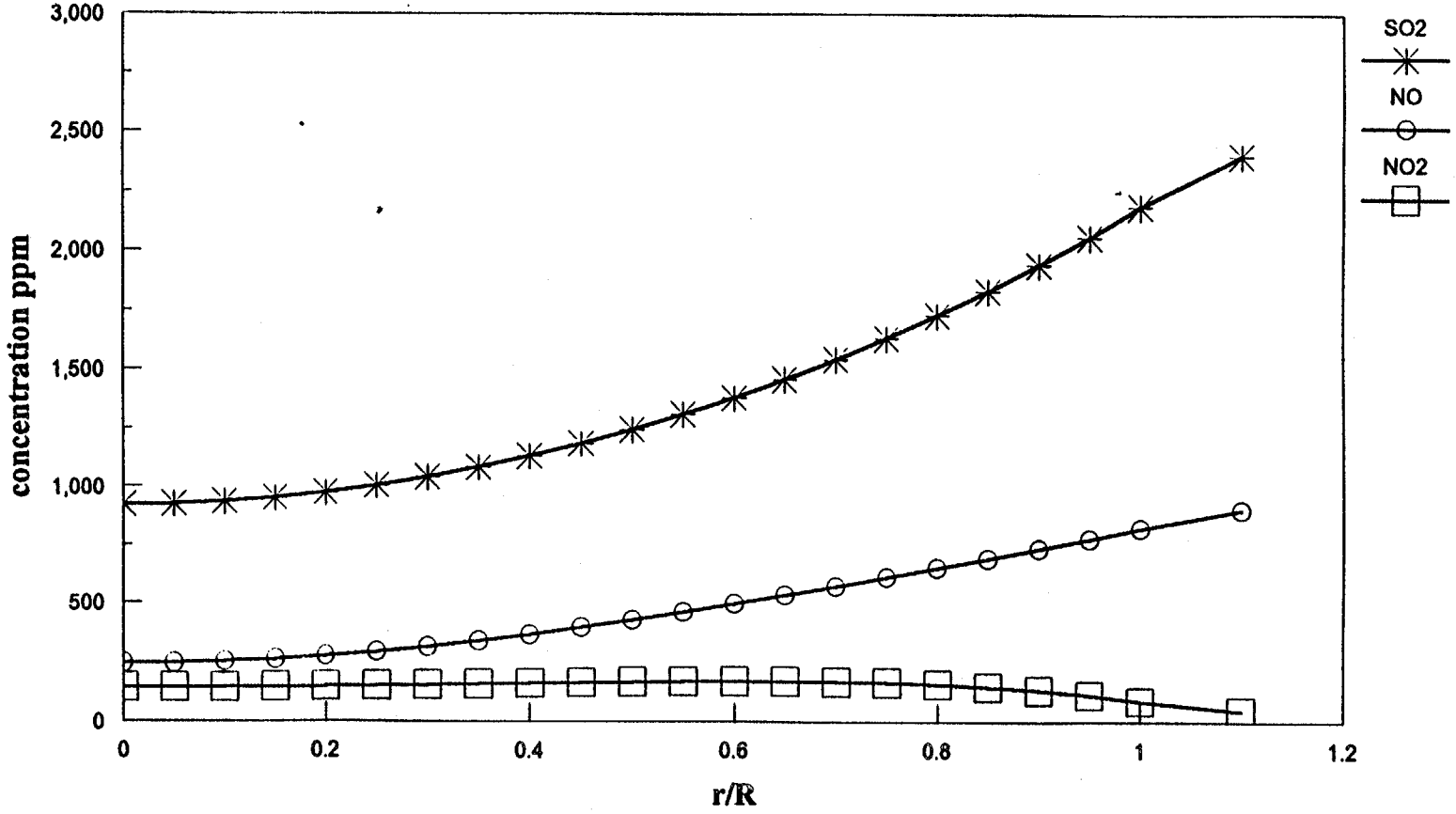

C:\may94\fixbed\ads\dos\GPFL15.cht

Figure 3-14.

Gas concentration profile inside the sorbent

(after 30 min)

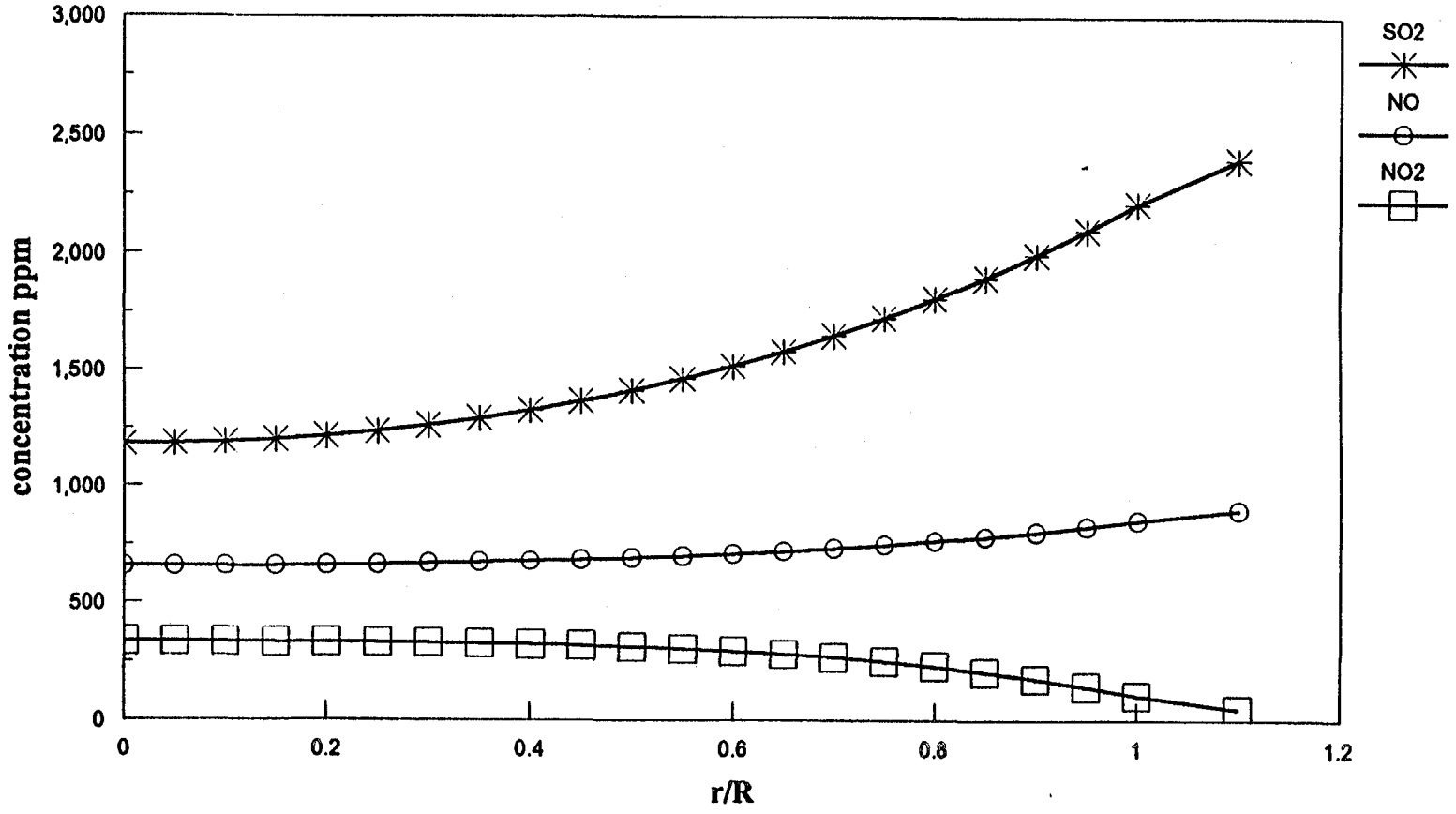

C:\may94\fixbed\ads\dos\GPFL30.cht

Figure 3-15.

Gas concentration profile inside the sorbent

(after 45 min)

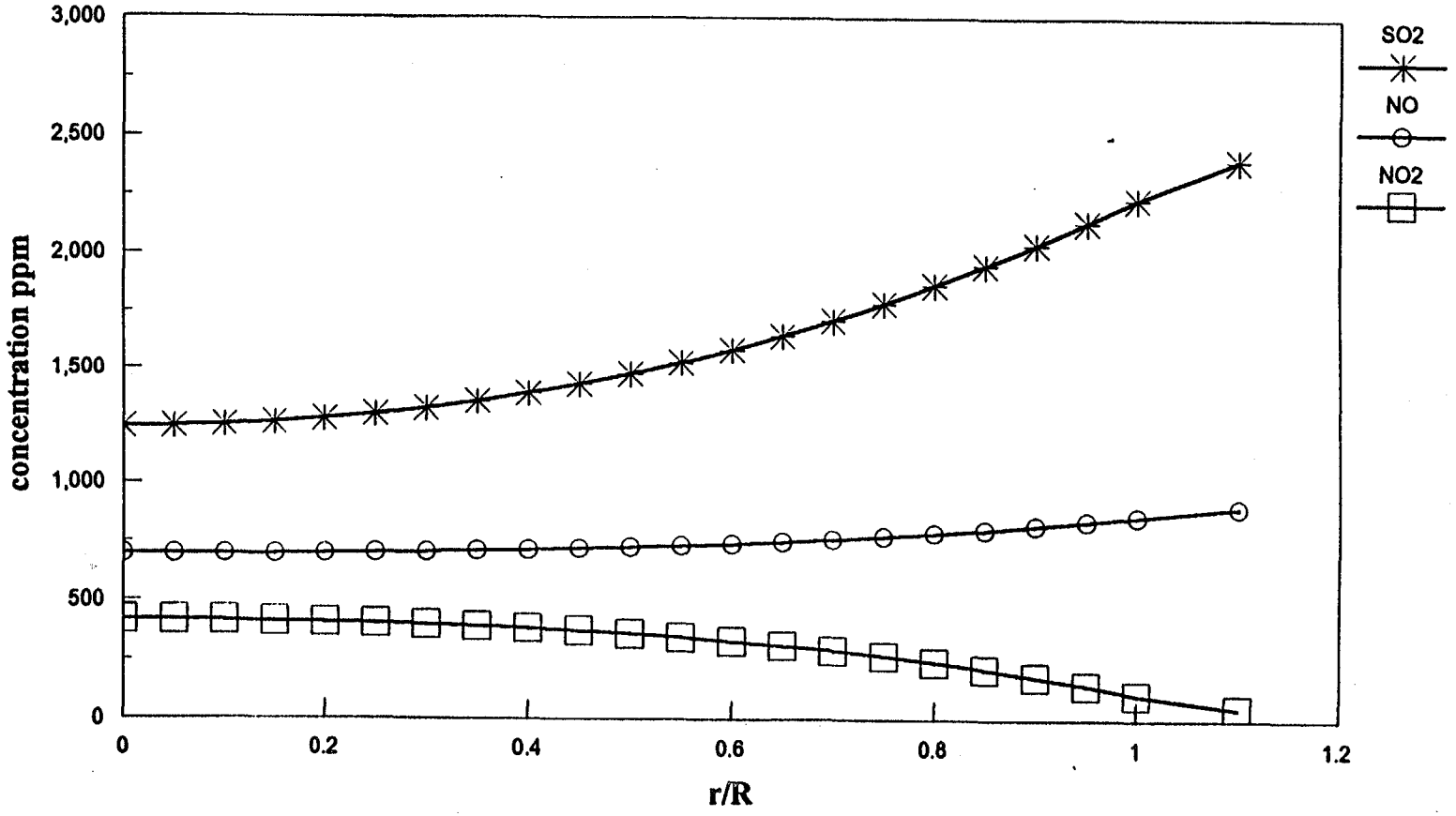

C:\may94\fixbed\ads\dos\GPFL45.cht

Figure 3-16.

Solid concentration profile inside the sorbent

(after 15 min)

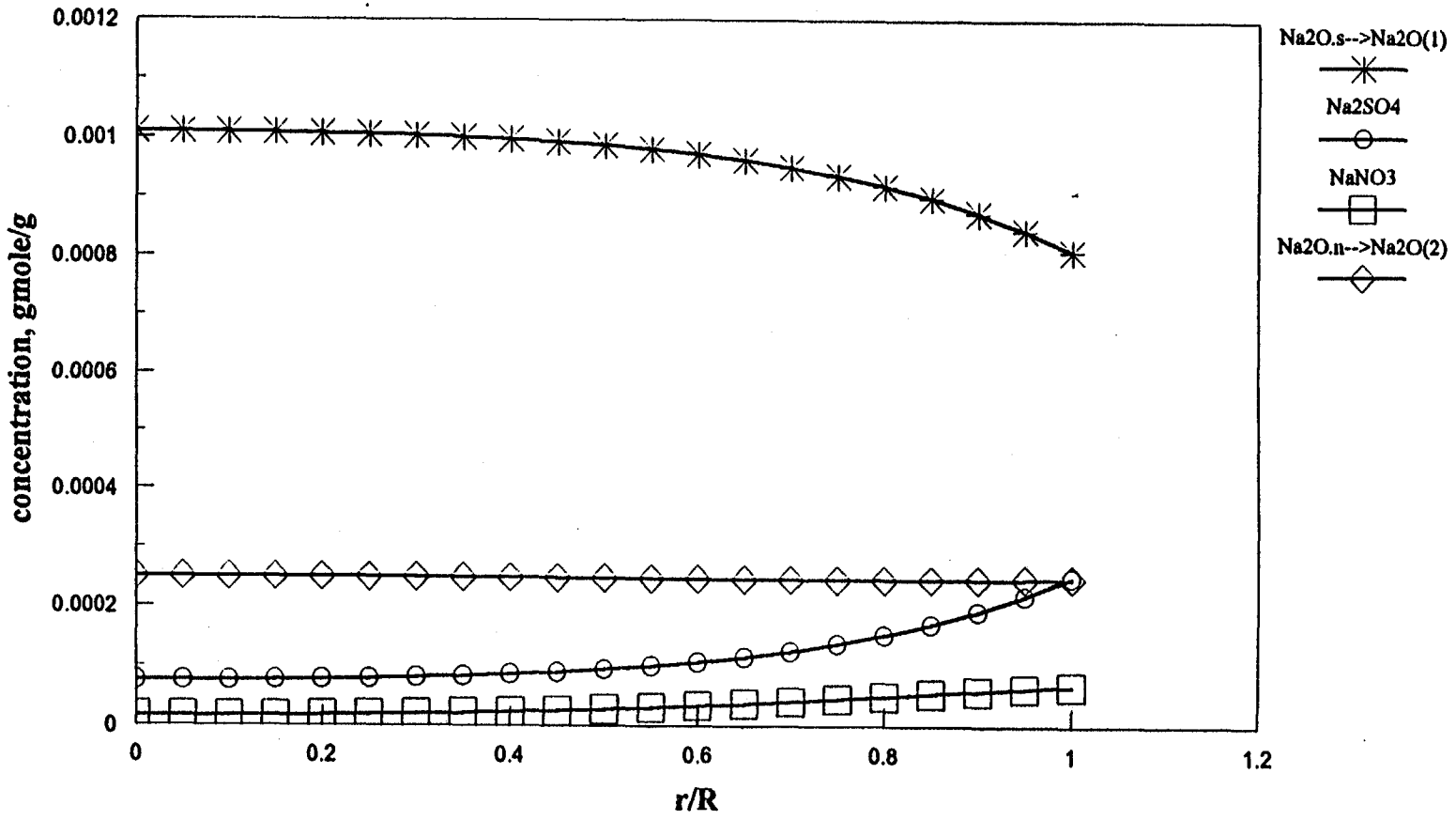

C:\may94\fixbed\ads\dos\SPFL15.cht

Figure 3-17.

Solid concentration profile inside the sorbent

(after 30 min)

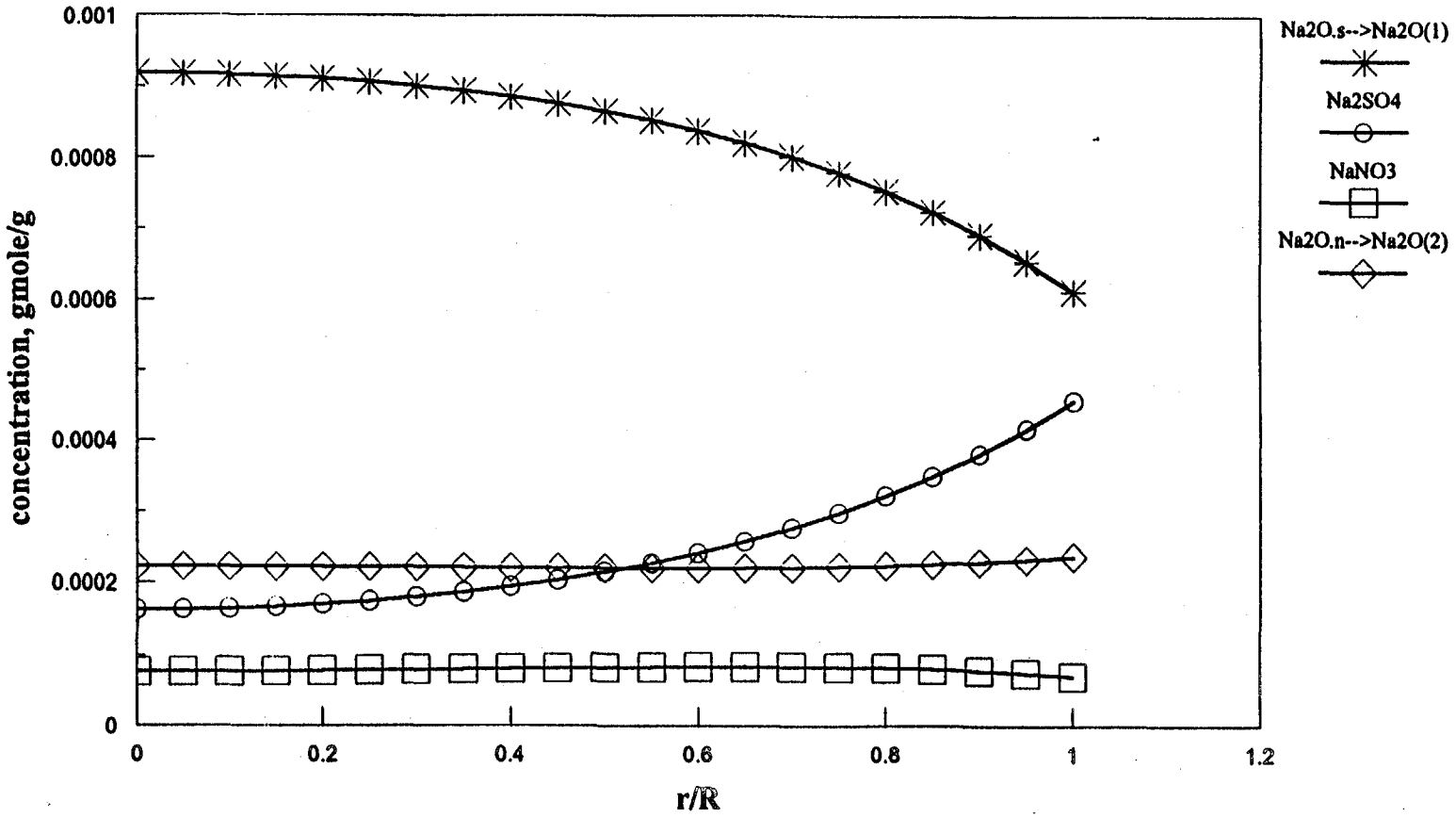

C:\may94\fixbed\ads\dos\SPFL30.cht

Figure 3-18.

Solid concentration profile inside the sorbent

(after 45 min)

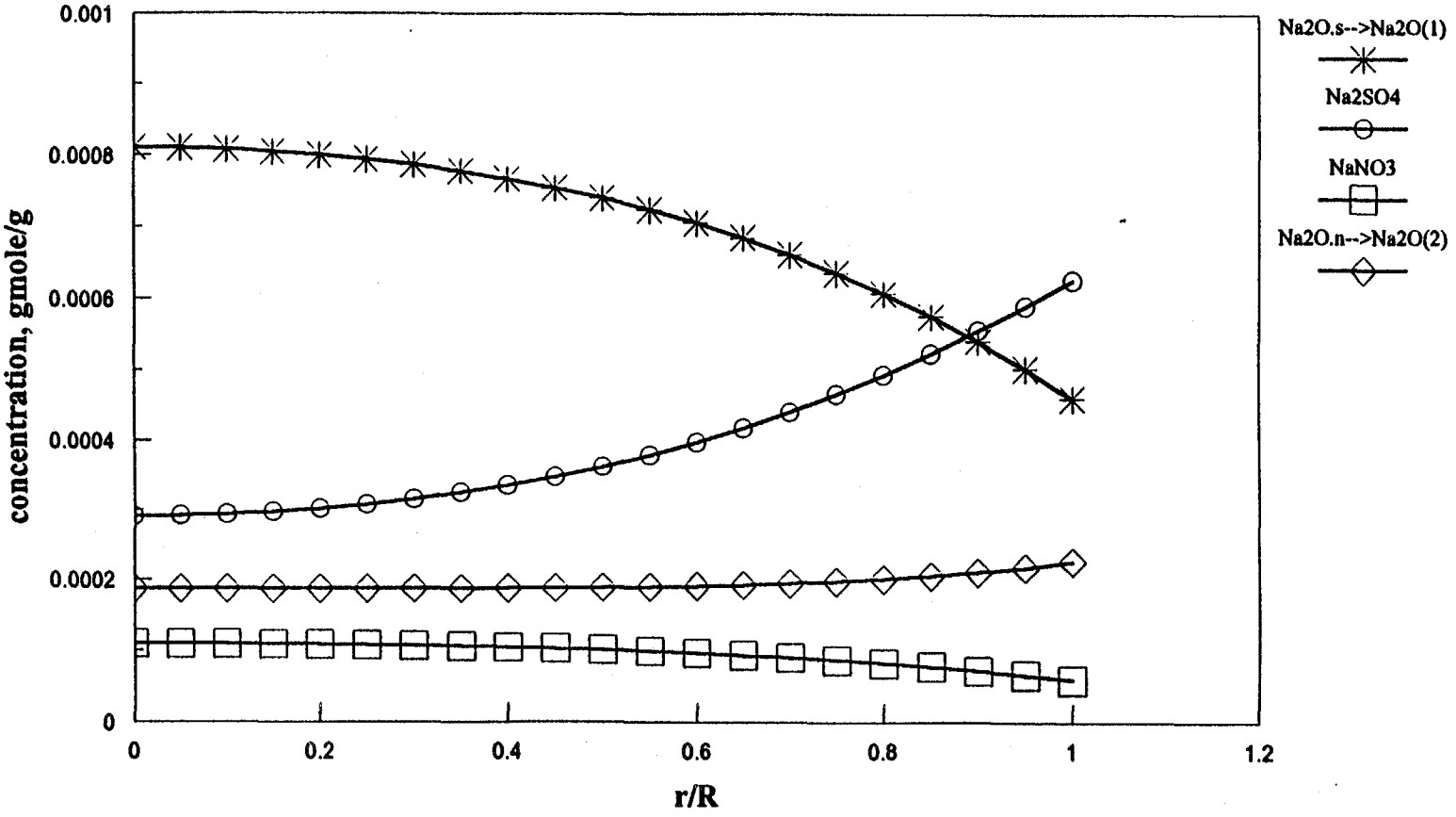

C:\may94\fixbed\ads\dos\SPFL45.cht

Inspecting the gas and solid concentration profiles inside the sorbent pellet reveals the following guidelines to improve NOXSO sorbent performance.

1. Use smaller particle size
2. Increase the sorbent porosity
3. Increase the alumina sorption sites by reducing sorbent silicate content.

Reducing the sorbent size cuts down the gas penetration time, which allows the center solid component to join the reaction earlier. Increasing the sorbent porosity also reduces the gas penetration time, which helps the sodium to react fast. POC-40 sorbent contains 6.8 wt% silicate to prolong the sorbent structure. But the presence of silicate makes sorbent substrate more acidic, which reduces the sorbent activity. Because of silicate the alumina sorption sites were reduced. A detailed discussion about the silicate effect on the NOXSO sorbent performance had been given in the POC final report.

3.5.2 Liquid SO_2 Production

As discussed in previous quarterly reports, the original plan was to make elemental sulfur from the regenerator offgas. However, the potential increase in sulfur by-product revenue by producing sulfuric acid or food grade liquid SO_2 made these options attractive. Additionally, site specific conditions may favor the production of sulfuric acid or liquid SO_2 over elemental sulfur. For example, the production of liquid SO_2 would be favored if an industrial use was nearby.

Based on the potential for increased revenue, it was determined that the production of liquid SO_2 from the regenerator offgas merited further attention beyond the Chemetics International reply. As discussed, in Quarterly Report #10, Chemetics International was unable to make marketable food grade liquid SO_2 from the regenerator offgas. A two-pronged approach including identifying commercially proven processes or designing processes to produce food grade liquid SO_2 from the regenerator offgas was initiated. Three potential processes were identified, one of which was a commercially proven process.

The commercially proven process was developed by Brown & Root Braun and, hereafter, will be referred to as the Claus burn process. Refer to **Figure 3-19**. A Claus process is used to produce elemental sulfur. The elemental sulfur is then pumped to a reactor where oxygen is introduced into a hot pool of molten sulfur where combustion occurs producing SO_2 gas. The excess heat produced by the combustion vaporizes additional molten sulfur. A waste heat boiler then cools the gas stream to approximately 800°F condensing the sulfur vapor and producing steam. The condensed sulfur is recycled back to the reactor. The SO_2 gas is then condensed and pumped to storage.

The processes designed to produce food grade liquid SO_2 are based on industry proven components, however, the integration of the individual components into a complete system is unique. The first designed process utilizes distillation to separate the SO_2 from N_2 and CO_2 in the gas stream. The regenerator offgas is initially incinerated, refer to **Figure 3-20**, to oxidize

Figure 3-19. Claus & Burn Process

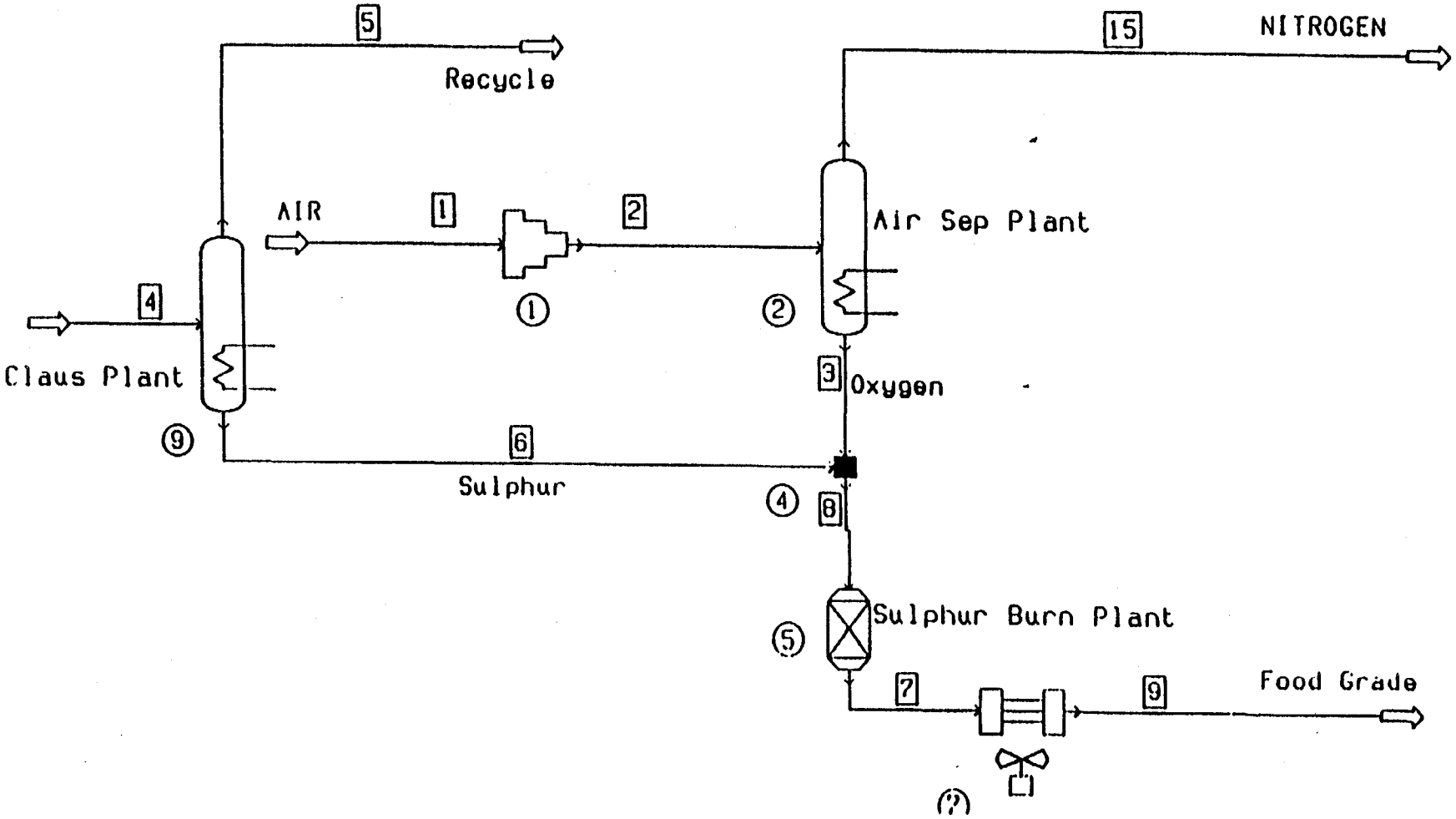

Figure 3-20. Distillation Option

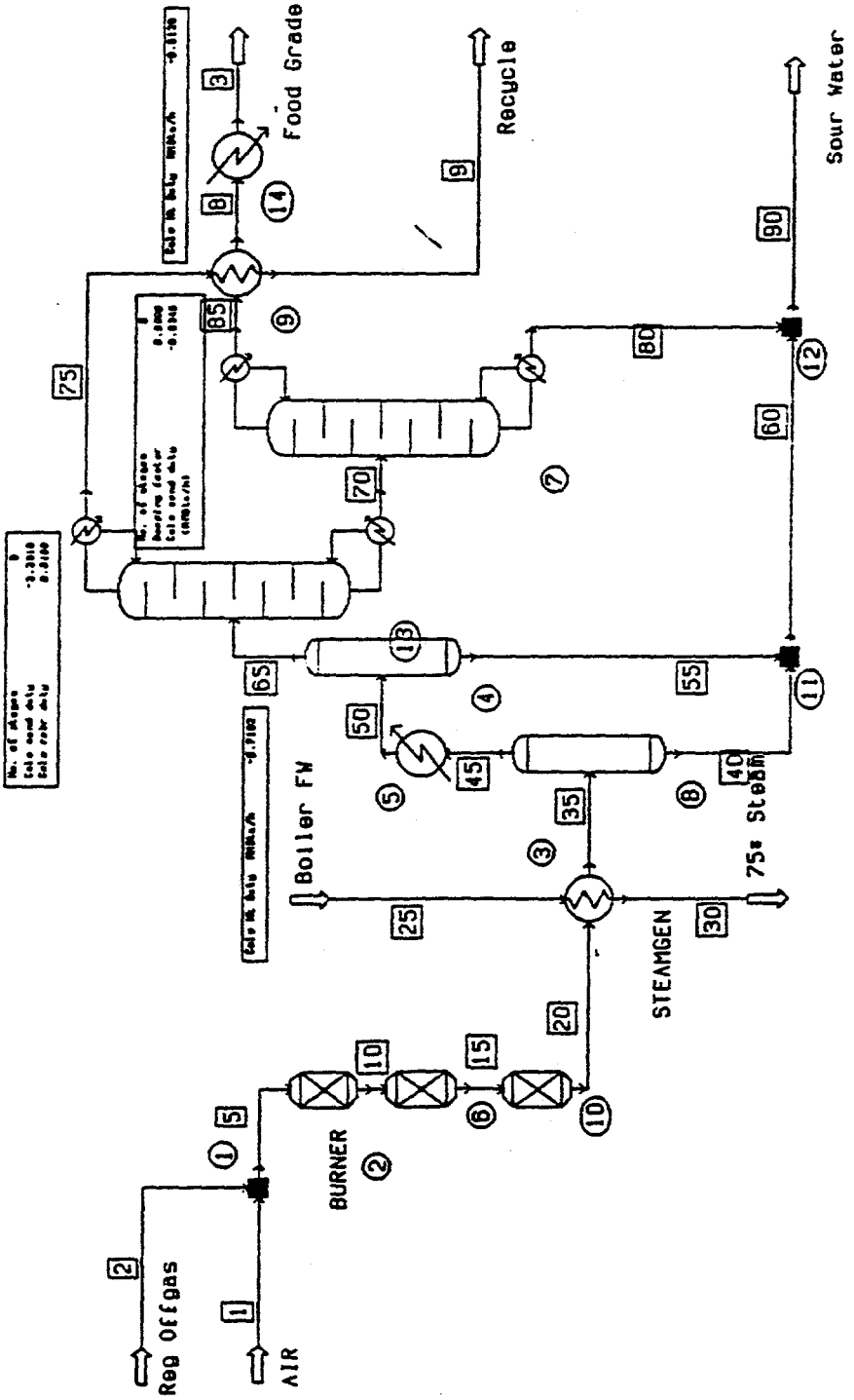

combustables to either SO_2 or CO_2 in the gas stream. Waste heat from the gas stream is recovered by producing steam. The gas stream is then cooled further to condense out most of the water. SO_2 gas is then separated from the dry gas stream using a series of two distillation columns. The SO_2 gas is chilled under moderate pressure to produce food grade liquid SO_2.

The second process designed to produce food grade liquid SO_2 from the regenerator offgas uses physical adsorption of SO_2 into a liquid to separate the sulfur dioxide from the SO_2 containing gas. The Union Carbide Selexol solvent was chosen as the stripping liquid due to the high solubility of SO_2 relative to CO_2. As in the other process, the regenerator offgas is initially incinerated to oxidize all combustables, refer to **Figure 3-21**, followed by a waste heat boiler which produces steam. The gas stream is then dehydrated to prevent the Selexol solvent from absorbing water. Both a glycol dehydration system and a chilled water system are under review for this application. The sulfur dioxide is then separated from the SO_2 containing gas using the Selexol solvent. The Selexol solvent is then heated driving off the sulfur dioxide. The sulfur dioxide gas is chilled under moderate pressure to produce food grade liquid SO_2.

Brown & Root Braun has supplied a budget level capital cost for a 70 TPD food grade liquid SO_2 plant. In addition, budget level costs for most of the major items of equipment for the designed processes have been received. At this time, it appears that the distillation system will have the lowest capital cost. The Selexol absorption system has the lowest operating costs. The Brown & Root Braun process has the highest capital and operating cost.

If the sulfur by-product of choice at the NOXSO commercial demonstration plant is food grade liquid SO_2, the process of choice to produce it would be the Claus burn process. While initially it appears that the designed processes are less expensive to purchase and operate, these designs are preliminary and require additional process engineering and optimization. At this time, the savings associated with the designs over the industry proven Claus burn process do not outweigh the associated risks of a first of its kind process. In addition, the Claus burn process provides the ability to produce elemental sulfur during periods of low food grade liquid SO_2 marketability and, more importantly, it provides Claus plant experience in producing elemental sulfur which would be the sulfur by-product of choice for most NOXSO installations.

3.5.3 Process Simulation

The process simulation model is being updated to reflect process changes and equipment rearrangement. For example, the methane treater and steam treater have been combined into a single vessel and the sorbent cooler to surge bin dense phase system has been replaced with L-valves.

Other improvements to the simulation program have been geared towards making the model more flexible and more accurately able to simulate real world conditions. As was shown in Quarterly Report #9, the gas flow rate required to heat or cool the sorbent in the sorbent heater or sorbent cooler vessels, decreases with increasing approach to plug flow on the counter-current stages in the fluid bed vessels. The sorbent heater and sorbent cooler subroutines have been modified to allow for the modeling of the fluid bed stages in these vessels as either a single

Figure 3-21. Selexol Option

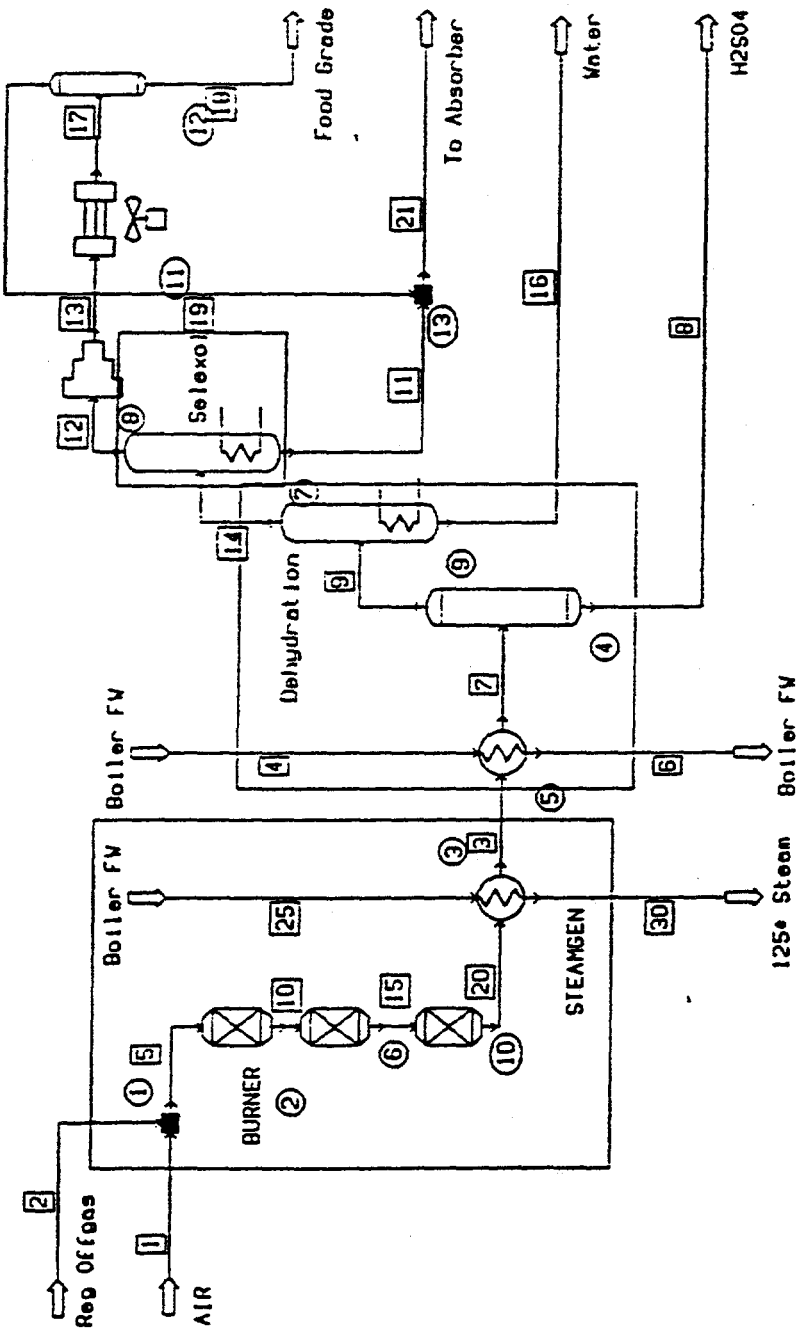

CSTR or any number of successive CSTR's in series simulating the approach to plug flow. The procedure used to calculate vessel dimensions has also been reworked. It now more accurately calculates the required vessel height by calculating the proper torispherical head height and, where applicable, the bottom cone height. Also, a new subroutine was written to calculate the convective and radiative heat loss from all of the process vessels.

3.5.4 HCl Adsorption/Desorption Characteristics

The HCl studies were started during this quarter. The tasks performed were

1. review of all previous laboratory and proof-of-concept data on HCl,
2. setup and calibration of lab equipment for HCl tests,
3. initial HCl lab tests,
4. examination of HCl reactions with NOXSO sorbent, and
5. compilation of alternatives for handling HCl within the NOXSO process.

NOXSO sorbent has been shown to be very efficient in removing HCl form flue gas. This data from the POC project in 1993 is summarized below:

Measurement	Date	Adsorber Removal Efficiency	Mass Balance Closure
Wet chemical	3/29-3/31	96.0%	66%
Continuous analyzer	7/19	96.6%	47%
Mass Spectrometer	7/19	97.5%	36%

The low mass balance closure is because not all of the HCl removed in the adsorber was measured in the sorbent heater offgas. The NOXSO sorbent used for the POC tests showed no accumulation of Cl during the project. This shows that Cl does not build up on the sorbent. Early lab tests (7/7/93) showed very high HCl removal efficiencies but only partial release of HCl from the sorbent on heating.

The process mass spectrometer was transferred to the NOXSO Clairton lab in August 1993. A control board for the analyzer was repaired in September and the analyzer calibrated for analysis of HCl and Cl_2. Calibration gases for this analyzer are normally contained in argon, but nitrogen had to be used with HCl. (The HCl peak is at a m/e = 36, argon has an isotope at the same peak location equal to 0.337% of the argon). Other difficulties were encountered with the addition of water to HCl containing gases. HCl is very water soluble and any condensed water within either the gas feed or analytical system removes HCl prior to analysis. This was overcome by redesigning the water feed system using a low flow positive displacement pump and by heating all gas lines above 230°F.

An adsorption/heatup test using sorbent beads and flue gas containing HCl was performed on 9/30/93. This test showed that:

1. SO_2 breakthrough occurred before HCl breakthrough in a fixed bed of sorbent,
2. upon heatup the HCl and NO_x evolve in the same temperature range,
3. some Cl_2 evolves from the sorbent during heatup, and
4. no other forms of Cl other than Cl_2 and HCl seem to be present during sorbent heating.

Only part of the HCl evolved from the sorbent as the NO_x was released. Some of the HCl was observed desorbing slowly from the sorbent after heating above 900°F. This indicates that two distinct forms of Cl may be present on the sorbent. No Cl_2 was detected in the flue gas leaving the bed during adsorption. This test had a gas phase mass balance closure of 60%.

A major industrial process (the Manniheim process) for the production of HCl from NaCl and sulfuric acid was found in the chemical literature. The reactions are:

$$NaCl + H_2SO_4 = HCl + NaHSO_4 \quad (1)$$
$$NaCl + NaHSO_4 = HCl + Na_2SO_4 \quad (2)$$

Reaction #1 occurs at 302°F while reaction #2 occurs at 1022-1112°F. These reactions occur in the Manniheim process, where the reactants are indirectly heated to 1549°F. The Hargreaves process is a variation of the Manniheim process which uses SO_2, water, and air instead of sulfuric acid.

$$4NaCl + 2SO_2 + O_2 + 2H_2O = 2\ Na_2SO_4 + 4HCl \quad (3)$$

This reaction occurs at approximately 1000°F. Some of the Cl on the NOXSO sorbent is probably as NaCl. The reactions between NaCl and sulfuric acid (or SO_2, H_2O, and O_2) are a possible explanation for chlorides not accumulating on the sorbent. The Gibbs free energy for reactions 1, 2, and 3 are negative over the entire temperature range and cannot be used to explain the removal of HCl from the flue gas.

The net effect of chlorides within the process as applied to coal combustion flue gas was examined. Every 0.1% Cl in coal produces approximately 80 ppm HCl in flue gas. Only 4% of Cl in coal stays with the coal ash with the remained converted to HCl. Most American coals contain less than 0.1% Cl while some coals (in Illinois and western Kentucky) have up to 0.65 Cl%. HCl levels less than 200 ppm in flue gas are regarded as having a negligible effect on boiler corrosion rates.

Experimental data has shown the NOXSO sorbent is effective at adsorbing HCl. Tests results also show that the adsorbed chlorides do not accumulate on NOXSO sorbent, but desorb when heated to regeneration temperatures. Although the NO_x and chlorine (HCL and Cl_2) start to evolve in the same temperature range, the HCl continues to come off the sorbent after all of the NO_x has desorbed. In the demonstration plant, hot sorbent from the sorbent heater will be

transferred by a L-valve to a steam disengaging vessel. Sufficient HCl will be desorbed in the steam disengaging vessel to use this as a convenient method for removing chlorides from the NOXSO process.

3.5.5 Attrited Sorbent Particles Size Analysis

Attrited sorbent particle size distribution tests were performed by Envisage Environmental Inc., at the POC and by the NOXSO lab. The results of these tests indicate that the majority of the attrited sorbent is 10 micron and smaller, contrary to previous data. Based on this latest data, the demonstration plant adsorber cyclone performance was re-evaluated.

Envisage Environmental Inc., an independent testing laboratory, made measurements of particulate loadings and size distribution at three points in the NOXSO POC plant. The three points were sorbent heater outlet, adsorber inlet and adsorber outlet downstream of the cyclone. Data from the sorbent heater outlet sampling was chosen to re-evaluate the cyclones for the demonstration plant.

The measured particulate concentration in the heater offgas stream was 0.034 grains/ft^3 of gas. Using the cyclone grade efficiency curve supplied by the manufacturer and the measured particle size distribution, a removal efficiency for the attrited sorbent is determined, see Table 3-8.

Table 3-8. Particle Size Distribution and Cyclone Removal Efficiency

Particle size (micron)	% in Range	Separation Efficiency %	Removal Efficiency %
13.6 & larger	6.3	96	6.0
8.5-13.6	1.8	93	1.7
5.8-8.5	21.7	85	18.4
4.0-5.8	15.9	76	12.1
2.6-4.0	43.0	63	27.1
1.3-2.6	4.0	45	1.8
less than 1	7.3	0	0
Total	100		67.1

Using the cyclone removal efficiency of 67.1% and the inlet loading of 0.034 grains/ft^3. The outlet loading is found to be 0.011 grains/ft^3. Specifications for a typical ESP require an outlet loading not to exceed 0.024 grains/ft^3. In terms of firing rate 0.011 grains/ft^3 would be equivalent to 0.04 lbm/MMBtu. A typical particulate emission permit limit is 0.1 lbm/MMBtu.

Envisage Environmental Inc. used EPA method 5 for particulate measurements. This method requires a measurement of the flow rate in the duct at the sampling point. This measured flow rate is then used to set the isokinetic sampling rate. Envisage's measured flows were consistently higher than NOXSO's measurements and in the case of the heater the flow that they measured was greater than the maximum output of the fan. This would lead to a sampling rate greater than isokinetic and measured particulate loadings higher than actually present. If this is true, then the outlet particulate loadings would be less than the values shown in the previous paragraph. However, since the Envisage values are the best independent measurements available, they will be accepted for the cyclone evaluation.

If it is necessary to achieve a higher cyclone removal efficiency, this can be accomplished by drawing a purge flow on the primary cyclone dust outlet ports. A purge flow of 10% of the primary cyclone throughput is drawn from the dust outlet ports through a secondary high efficiency cyclone by a fan that discharges back to the inlet of the primary cyclone. The purge flow draws more of the finer particulates out of the primary cyclone where they are removed in the high efficiency cyclone. The fans required are 35 H.P. each which would cause an electrical power increase of 3½% for the process. A quantified performance improvement with the secondary flow has yet to be determined.

3.5.6 Sorbent Heater/Cooler Energy Balance

During the operation of the recycle system at the POC, optimization studies examined the effect of varying the sorbent residence times in the heater and cooler. The data analysis identifies the effects on plant operations and on the energy balances around the sorbent heater and cooler.

Varying Bed Level Heights

The heat transfer between the gas and the solids in a fluid bed is considered to be very fast. Fast enough such that the gas and solids temperatures can be assumed to be equal as they exit the bed. As a result, the sorbent residence times in the sorbent heater and cooler were not a concern in the design of the pilot plant with regard to heat transfer. But from an economic point of view, the shorter the sorbent residence time in the fluid bed the better. Shorter time in the sorbent heater and cooler implies less sorbent inventory because the sorbent circulation rate is determined by the adsorber's SO_2 removal requirement. High sorbent inventory demands more fan power to fluidize the sorbent. It also increases the sorbent attrition and requires more sorbent to fill the system. However, a minimum amount of sorbent must be maintained in the fluid bed to prevent the gas from channelling through the bed and to allow the gas and sorbent temperatures to reach equilibrium before exiting the bed.

Sorbent Residence Times

In the POC final report, a mathematical model which predicts the sorbent residence times and temperatures was derived using data from the sorbent cooler. This model was then used to predict the minimum residence time required in the sorbent heater and cooler in order for the

necessary heat transfer to take place. The result of this analysis was the determination that a residence time of 200 to 300 seconds per stage should be long enough to accomplish the heat transfer while still providing enough sorbent in the fluid beds to prevent channelling of the gas.

Table 3-9 shows the POC sorbent heater residence times for various sorbent flow rates and heater expanded bed heights. The sorbent heater at the pilot plant had twelve inch overflows installed, hence, twelve inch expanded bed heights. As seen in the table, this bed height provided residence times two to three times longer than the analysis suggested was necessary. It was decided to operate the sorbent heater with nine inch and then six inch overflows, which provided residence times much shorter than had previously been employed. The overflows in the cooler were also changed to be nine inches high, but the heat transfer analysis focussed on the sorbent heater where the inlet sorbent and gas temperatures were able to be controlled.

Table 3-9. Sorbent Heater Residence Times

Solids Flow Rate, lb/hr	Expanded Bed Height		
	6"	9"	12"
7000	404	605	807
8000	353	530	706
9000	314	471	628
10000	282	424	565
11000	257	385	514
12000	235	353	471

Time, in seconds, that the sorbent spends at each stage within the heater

Testing Procedures

The ultimate purpose of the sorbent heater is to heat the sorbent to its regeneration temperature. The Distributed Control System (DCS) at the pilot plant controlled the sorbent heater's bottom bed temperature by changing the inlet gas temperature and mass flow to establish the desired sorbent temperature. The minimum gas mass flow was determined by the cooling requirements of the sorbent cooler. As such, the incoming gas temperature was the main control point for the sorbent heater, changing under the command of the DCS to ensure that the proper temperature was attained before the sorbent reached the regenerator. The other variables which were important to this analysis include the sorbent inlet temperature, sorbent mass flow, and the gas exit temperature. All of the variables were continuously monitored and collected for analysis by the DCS.

The varying overflow tests took place in May, June and early July after the power plant was shut down. During May, before the flue gas recycle system was complete, the pilot plant ran hot, inert flow tests with the twelve inch overflows still in place. When the pilot plant was shut down at the end of May to complete the duct tie-in for the flue gas recycle system, the nine inch overflows were installed in the sorbent heater and a specific test matrix was defined as shown in Table 3-10. The test program called for establishing the sorbent mass flow rate, sorbent entrance temperature at the heater, and the gas entrance temperature. The gas mass flow was then adjusted to attain the desired sorbent exit temperature while the gas exit temperature was also continuously monitored. The test matrix called for running the pilot plant at steady state for twenty four hours at each of the four test points with the nine inch overflows in place. Upon completion, the overflows were changed to six inches and the same test matrix was run again. The twelve inch overflows were not reinstalled and run under the test matrix conditions because of time constraints.

Table 3-10. Overflow Test Matrix

Sorbent Entrance Temperature, °F	Sorbent Exit Temperature, °F	Sorbent Mass Flow, lb/hr	Gas Inlet Temperature, °F
280	1150	8000	1330
280	1150	10000	1330
280	1150	10000	1390
280	1150	12000	1390
Matrix run for 9" then 6" overflows			

Test Results

The immediately perceptible result of the test was the ability of the sorbent heater to successfully heat the sorbent to regeneration temperature even with the reduced residence times. Proper operation of the plant was easily maintained with the six inch overflows in place, and no other adjustments in the control system or elsewhere, were needed for the sorbent heater to perform its task. The data analysis was then left to decide how efficiently the heater performed under the various conditions.

One parameter which can be used for comparison is the efficiency of heat utilization. The efficiency of heat utilization of the gas is defined as follows:

$$\eta_g = \frac{Tg_i - Tg_o}{Tg_i - Ts_i}$$

where Tg_i is the gas inlet temperature, Tg_o is the gas exit temperature, and Ts_i is the sorbent inlet temperature. This parameter is significant in that it is a measure of the system's ability to

effectively use the heat being carried by the gas stream. It makes use of the gas exit temperature which was not constrained.

In **Figure 3-22**, the measured efficiency of gas heat utilization is plotted against the ratio of gas mass flow rate to sorbent mass flow for all of the test data and the twelve inch overflow data that had been collected immediately before the nine inch overflows were installed. The twelve inch data pattern is different than the other data because of the varying test parameters. The lines in the graph represent a best fit linear regression generated by a least squares analysis and its error band, plus or minus ten percent of the linear fit. All of the data falls within this error region which, when considered with the interspersing of data, suggests that six inch overflows are just as effective as twelve inch overflows for heat transfer. But the data analysis does not end with the qualification of six inch overflows in the design considerations of future plants.

Figure 3-23 is a plot of the heat gained by the sorbent versus the heat lost by the gas for the same set of data from **Figure 3-22**. Again, the lines in this graph represent a best fit linear regression and its error band, plus or minus ten percent. The significance of this graph is the intercept of the best fit line with the y-axis. Because the gas always lost more heat than the sorbent gained, this intercept represents the heat lost to the surroundings. The results estimate the heat loss to be approximately 800,000 Btu/hr, over one quarter of the heat lost by the gas stream. A previous analysis estimated the amount of heat lost through the heater walls of approximately 35,000 Btu/hr which, it is felt, is a reasonable estimate. But considering the fact that it is an order of magnitude lower than the measured loss, coupled with the fact that all of the data from **Figure 3-23** does not fall within the error region, suggests that the mechanism at work here is not as simple as heat lost to the environment.

Figure 3-24 plots the measured efficiency of gas heat utilization versus the theoretical efficiency. The theoretical efficiency was computed assuming that all of the heat lost by the gas was gained by the sorbent, the gas exit temperature was then calculated for this case and used to evaluate a theoretical efficiency of gas heat utilization. The significance of the graph is that the measured efficiency is always higher than the theoretical efficiency, in other words, the gas is always losing more heat than is necessary to heat the sorbent to the desired temperature. To explain this, it is proposed that the sorbent carries water on it into the heater. Some of the heat in the gas stream is then used to drive the water off. The desiccant properties of the sorbent had been previously observed, but not quantified; however, the deficient energy balance closures experienced at the POC support this proposition.

POC Energy Balance Closures

The energy balance closures around the sorbent heater and sorbent cooler at the POC had always been deficient, with results in the 70-85% range for the heater and 80-90% range for the cooler. This energy imbalance was evident throughout POC testing. At first, this deficiency was believed to be due to deviations in the sorbent and air mass flow rate measurements. The MAC dense phase transport system, for instance, used capacitance level probes which were

Figure 3-22. GAS HEAT UTILIZATION EFFICIENCY

ALL DATA

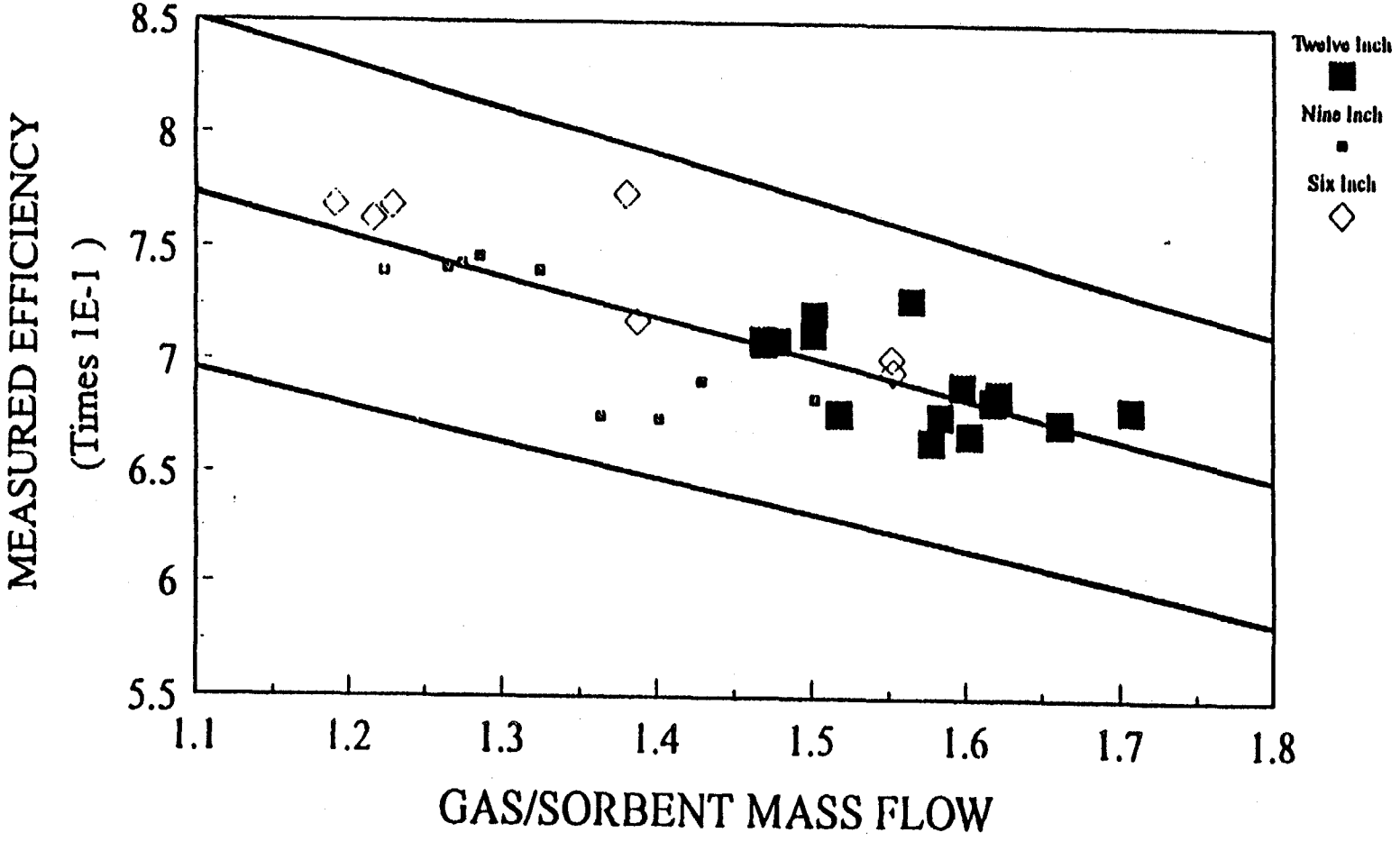

Figure 3-23. HEAT TRANSFER

ALL DATA

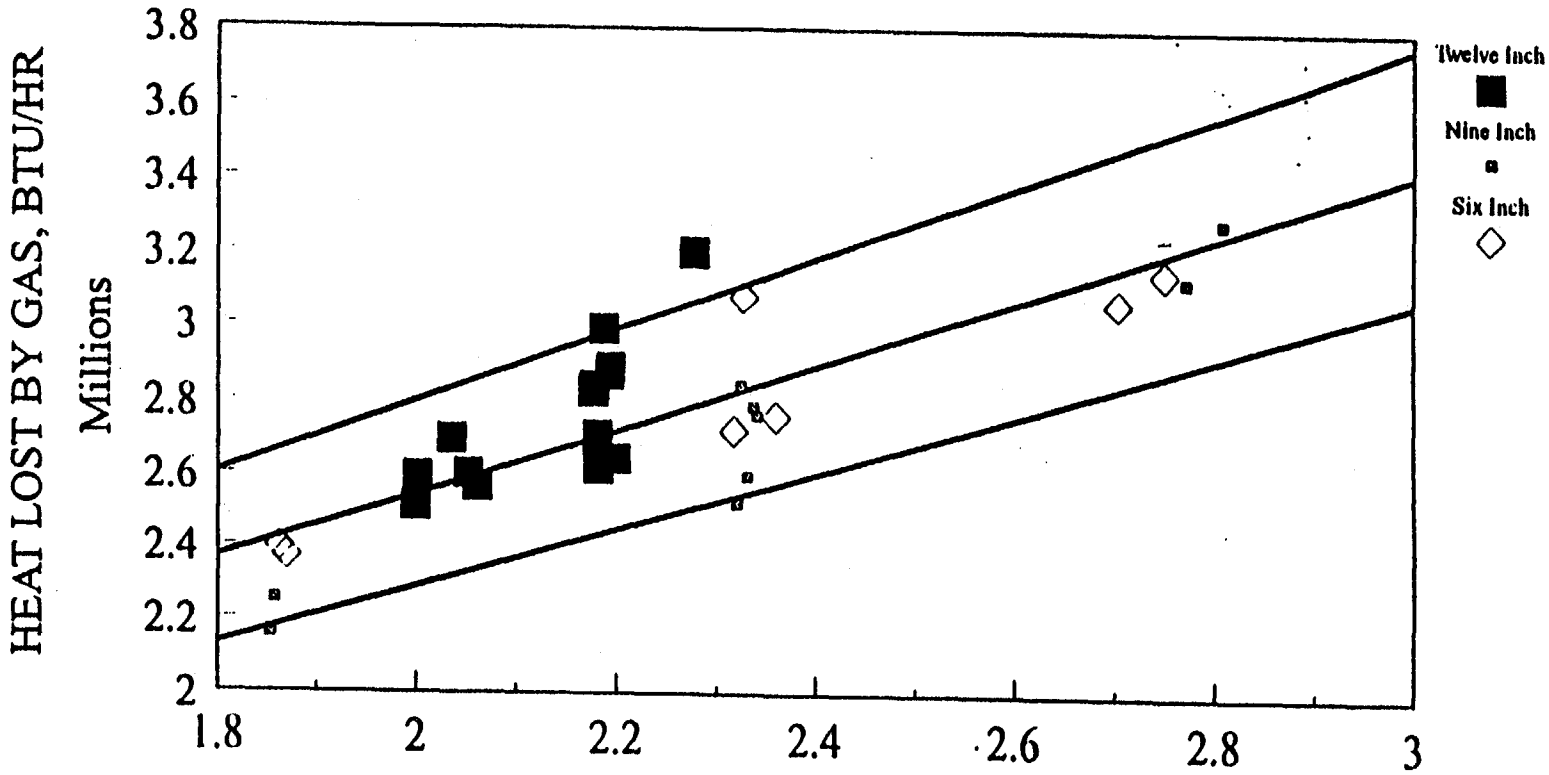

Figure 3-24. GAS HEAT UTILITZATION EFFICIENCY
ALL DATA

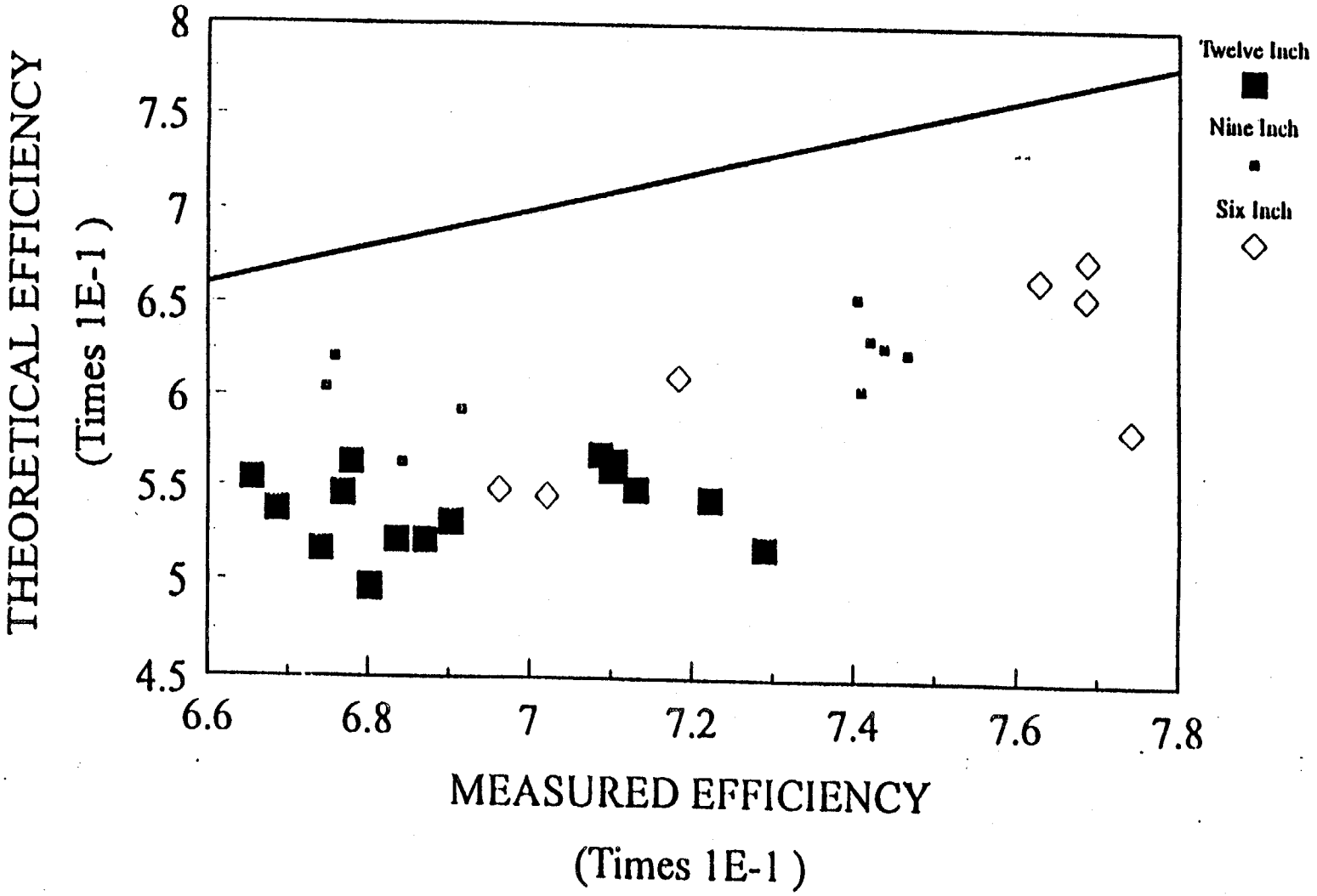

prone to calibration drift, resulting in variant batch sizes which effected the recorded sorbent mass flow rates. This variance could not be quantified, but the air mass flow rate provided some idea of how much this inconsistency may have affected the closures.

The air mass flow rates were measured at the entrance and the exit of the sorbent heater/cooler train. The air flow rate into the cooler and the cooler bypass were measured using turbine flow meters, which were consistent when they were operating. These meters experienced failures resulting in replacement of the turbine internals, but by the time of the sorbent heater bed depth tests, neither of the inlet readings were reliable so that the air flow rate measurements were made using the thermal dispersion meter at the sorbent heater exit. This flow rate measurement was later tested using a helium tracer test which showed the thermal dispersion readings to be 10% high and temperature dependant. As was expected, the corrections which resulted from this test did not resolve the energy balance closure deficiency. In fact, the closures reported above include this correction.

Uncertainty Analysis

In order to more fully quantify the deficiency in the energy balance closures an analysis to identify the uncertainty in the calculated closures was undertaken. This analysis was based on the second power equation developed by Kline and McClintock. (Kline, S.J. and F.A. McClintock, Describing Uncertainties in Single Sample Experiments, Mechanical Engineering, January, 1953.) The method estimates the uncertainty in the calculated result, in single-sample experiments, on the basis of the uncertainties of the primary measurements. The primary measurements, in this case, were the mass flow rates and the inlet and outlet temperatures of the sorbent and the fluidizing air. In order to implement the second power equation, the uncertainty in the primary measurements were stated as specifications given with certain odds. For instance, it was believed that the temperatures measured at the POC had 20 to 1 odds of being within 5 degrees of the recorded value. If all of the primary uncertainties are given with the same odds, the uncertainty in the result with the same odds can be calculated.

This analysis showed the mass flow rates to be the sources of the greatest amount of uncertainty. The air mass flow rate was estimated to be within 5% of the measured values, while the sorbent mass flow was estimated to be within 10% of the recorded values. Both of these high degrees of uncertainty result in the closure having an uncertainty of 11% of the calculated values. By including an analysis of ambient heat losses, the energy balance closures improved only slightly while the uncertainty was unaffected. The results of this analysis suggest that while the mass flow rate measurement variations do affect the energy balance closure, they are not the primary source of the energy imbalance, which further supports the water adsorption proposal.

To further qualify this proposal, another uncertainty analysis was undertaken. This time the objective of the analysis was to estimate the amount of water desorption which would be necessary in the sorbent heater in order to attain perfect closure based on the recorded process measurements. The analysis showed that changes in the sorbent water loadings of between 1% and 7% by weight from the heater entrance to the heater exit would be enough to fulfill the

closure. Comparisons of similar alumina products, available are on the market for applications, desiccant applications, suggest that this is a realistic water loading. Therefore, the results do qualify water desorption as a possible solution to the energy imbalances; however, the only way to verify this aspect is by producing adsorption isotherms for NOXSO's sorbent, which are not yet available. If water desorption can possibly resolve the energy imbalance in the sorbent heater, what of the energy imbalance in the sorbent cooler?

Cooler Energy Balance

As stated previously, the energy balance closures around the sorbent cooler were also deficient at the POC. While the cooler closures were better than the heater closures, they were still not within range of acceptable deviations. Contrary to the heater, the gas exiting the cooler was always hotter than it should have been after cooling the sorbent. It is proposed, in this case, that water is adsorbed in the sorbent cooler, evolving heat during the adsorption process. An analysis similar to that performed on sorbent heater data showed that sorbent water adsorption of up to 5% by weight inside the cooler would be enough to satisfy the closure requirements, assuming that all of the other measurements were accurate.

As was the case with the sorbent heater, the closure around the sorbent cooler was subject to the uncertainty within the primary measurements. This is more profound in the case of the cooler because in the case of the heater the air mass flow rate was measured by the thermal dispersion meter at the heater exit. This flow measurement is invalid for the cooler for all data generated with the cooler bypass open. This proved to be a problem when the turbine meters measuring the inlet flows failed. Eventually the cooler bypass was kept closed so that the exit gas flow rate measurement could be used for the cooler also.

To examine the effects of inconsistent measurements, **Figure 3-25** plots the cooler closure versus the heater closure for all data during the operation of the recycle system after the cooler bypass was closed. The linear nature of the graph suggests that there is an error in the measurement of at least one variable; however, the energy balance closures are beyond the affect of one or two variables. The next step in the analysis is to expand the data base to include data generated before the flue gas recycle system. This should minimize the effect of incongruous variables so that the effect of water adsorption and desorption on the sorbent can be better isolated and quantified. This analysis has also lead to further testing of NOXSO's sorbent desiccant properties, and eventually adsorption isotherms will be required to accurately account for this phenomenon in the design of the heater/cooler train, including the vessels and the air heater between them.

3.5.7 POC Plant Disposition

On August 1, 1993, Ohio Edison closed the Toronto Power Plant and the POC test came to an end. NOXSO agreed to dismantle the POC and restore the site. Bids have been obtained from three sub-contractors, one of whom will perform this work. NOXSO is ready to award the sub-contract and begin work as soon as the DOE has agreed to the final disposition of the

Figure 3-25. ENERGY BALANCE CLOSURES

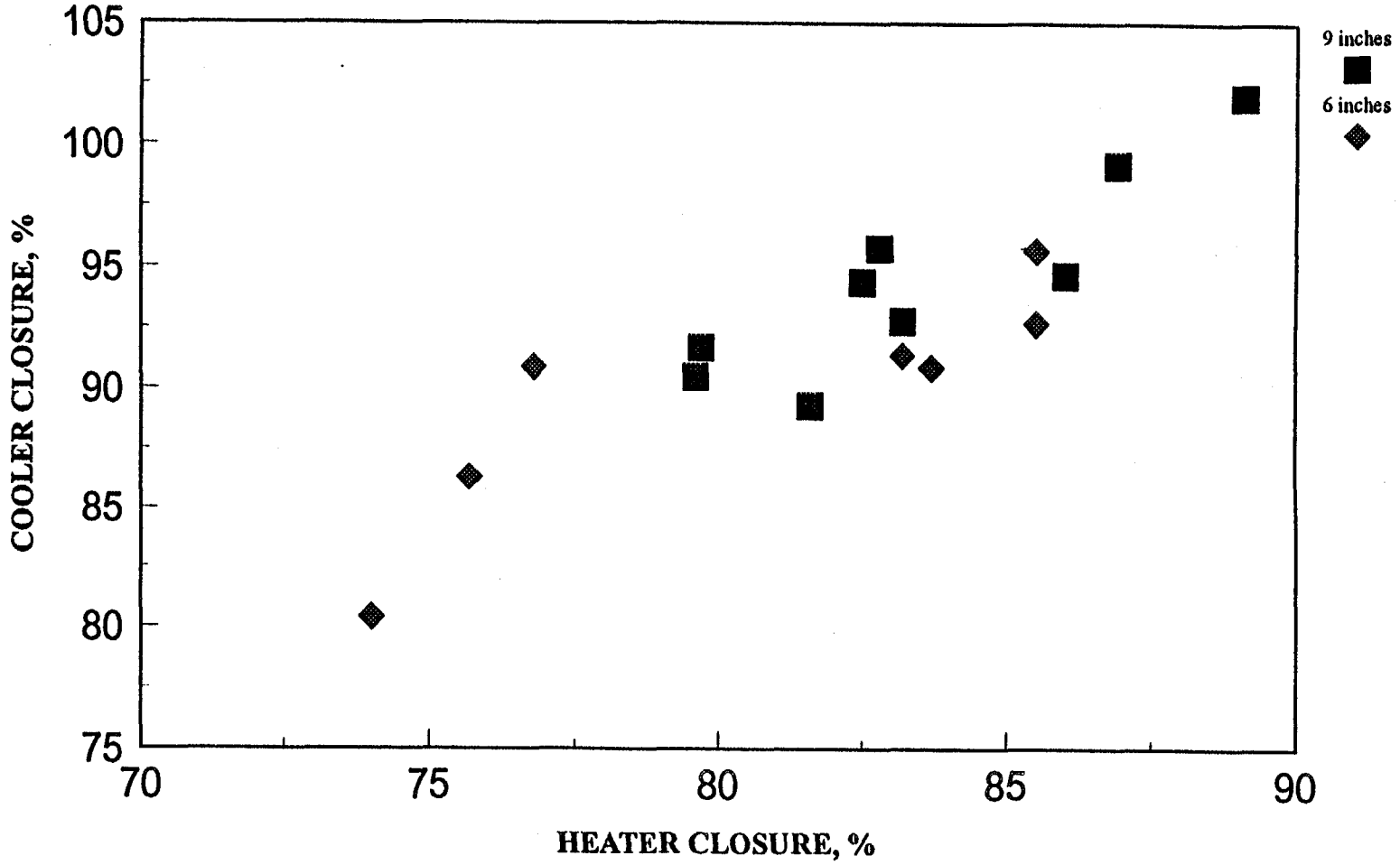

POC property. NOXSO submitted a POC property list to the DOE in September 1993. As soon as the DOE approves this list, NOXSO will begin the POC plant demolition and site restoration.

NOXSO had hoped to continue POC testing and consequently explored the possibility of moving the plant. The possibility of continued testing in Toronto, using bottled gases as was done in the last three months of the POC test was also explored. Until demolition begins, NOXSO will continue to explore these options. Although much was accomplished in the POC test, NOXSO sees benefit in continued POC testing since the work of process improvement is an ongoing effort.

3.6 Plant Characterization

Plant characterization activities are on hold until a new host site is identified.

3.7 Site Survey/Geotechnical Investigation

Site survey/geotechnical investigation activities are on hold until a new host site is identified.

3.8 Permitting

Permitting activities are on hold until a new host site is identified.

4.0 PLANS FOR NEXT QUARTER

The main priority for next quarter is the evaluation and selection of a host site for the project. It is essential that a technically acceptable site be selected so the process can be properly demonstrated.

Immediately upon identification of the host site, work will begin to modify the EIV with information specific to the new site. It is critical to satisfy the NEPA requirements as soon as possible to prevent this delaying the project,

With the decision made to use the scaled up POC design, emphasis will be shifted to reducing the height and cost of this design. Design flexibility is enabled by the fact that sorbent lift can be attained with the L-valves as demonstrated at the POC.

The need to perform additional NO_x destruction studies will be evaluated based on the boiler type for the new host site. However, since a significant data base of NO_x destruction efficiency versus boiler type currently exists, it is unlikely that additional experimental work will be required.

Plans to move the POC or continue operations using sythetic flue gas at the existing site have been unsuccessful. It is anticipated that demolition of the POC will begin this quarter.

The process studies which are ongoing in support of the commercial plant design will continue. The adsorber simulation program will be applied to high temperature sorption data to determine the reaction rate constants and corresponding alumina and sodium sorption sites. A proper temperature dependence will be obtained to satisfy both high and low temperature data. During the same period, a fluid-bed adsorber simulation program will be developed. POC data, which was obtained from fluid-bed reactor at different temperature, will be used to check the assumption about temperature dependence, reaction scheme, and gas-solid contact pattern in the fluid-bed.

Studies of the sorbent heater and cooler energy balance closure will continue. It is anticipated the failure to close the balance is due in large part to adsorption and desorption of water vapor on the sorbent. This effect will be verified and quantified to assure proper design of the sorbent heater and cooler at the commercial plant.

A thorough analysis of the pilot plant availability and causes of lost availability will be conducted. This will assure that all design deficiencies which caused lost availability will not be repeated in the commercial plant design. HCl lab tests will continue in the next quarter. These tests will measure 1) the HCl capacity of the sorbent, 2) the desorption gases produced on heating the sorbent, 3) the use of shallow beds of sorbent for HCl removal, 4) determine if HCl can replace SO_2 on the sorbent in the adsorber, and 5) reactions between HCl and alumina. The possible options for handing HCl within the NOXSO process will be evaluated.

As soon as a new host site is identified, activities to collect specific plant information, collect site and geotechnical information, and identify necessary permits will be initiated.